Supplementary Information

Regioselective Formylation of Rhenium-Oxo and Gold Corroles: Substituent Effects on Optical Spectra and Redox Potentials

Rune F. Einrem,[a] Einar Torfi Jonsson,[a] Simon J. Teat,[b] Nicholas S. Settineri,[b,c] Abraham B. Alemayehu,*[,a] and Abhik Ghosh*[,b]

[1]Department of Chemistry, UiT – The Arctic University of Norway, N-9037 Tromsø, Norway; Email: abraham.alemayehu@uit.no (ABA), abhik.ghosh@uit.no (AG)

[2]Advanced Light Source, Lawrence Berkeley National Laboratory, Berkeley, CA 94720-8229, USA

[3]Department of Chemistry, University of California, Berkeley, Berkeley, California 94720, USA

Contents **Page**

A. UV-vis spectra

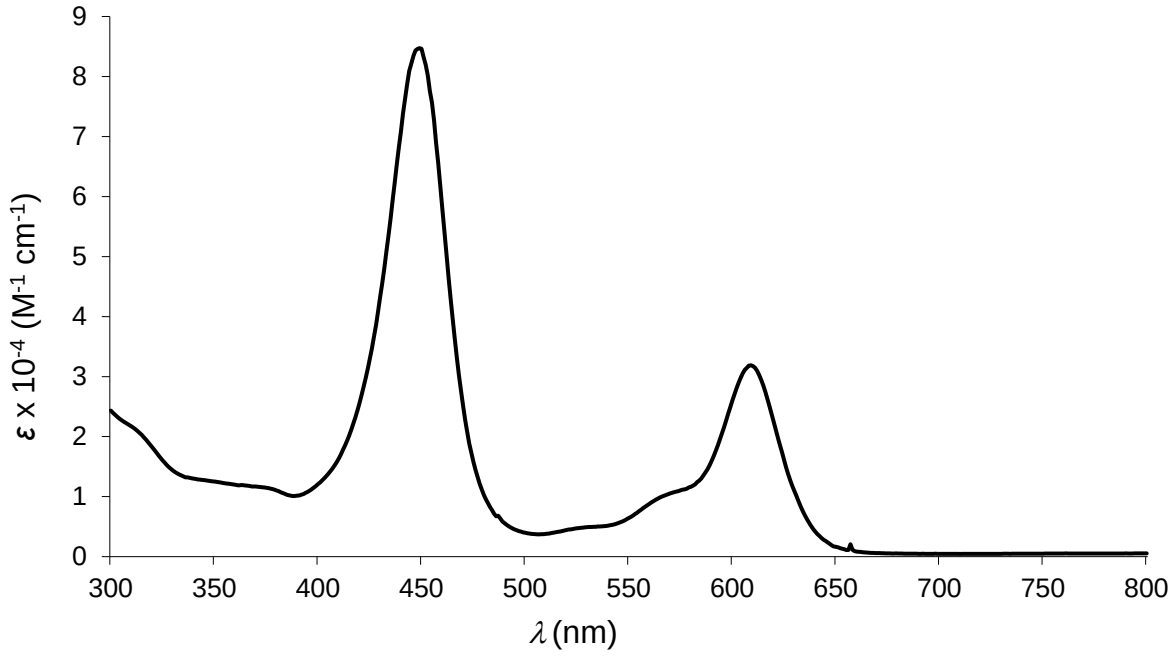

Figure S1. UV-vis spectrum of Re[TPC-3-CHO](O) in dichloromethane.

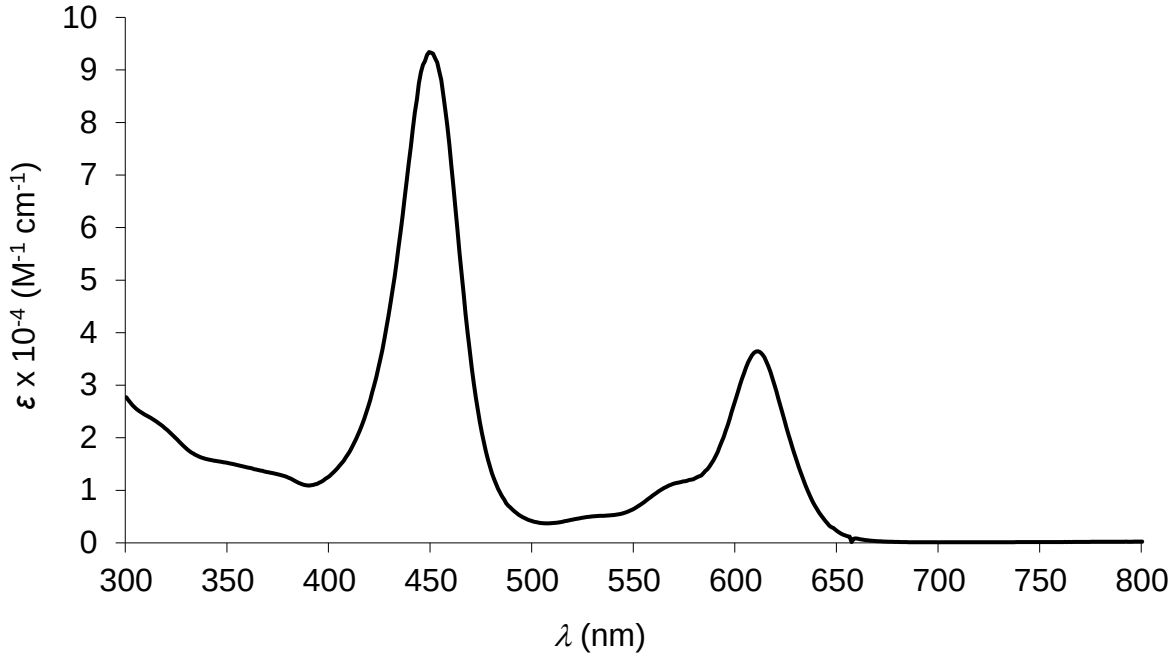

Figure S2. UV-vis spectrum of Re[T*p*CH_3PC-3-CHO](O) in dichloromethane.

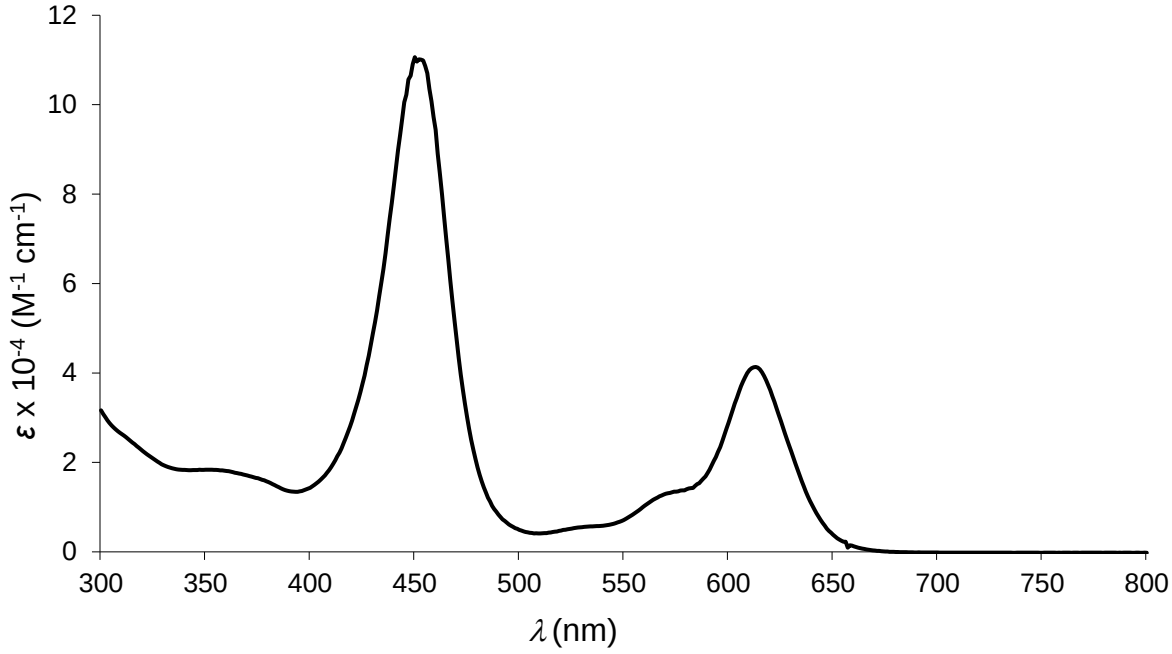

Figure S3. UV-vis spectrum of Re[T*p*OCH$_3$PC-3-CHO](O) in dichloromethane.

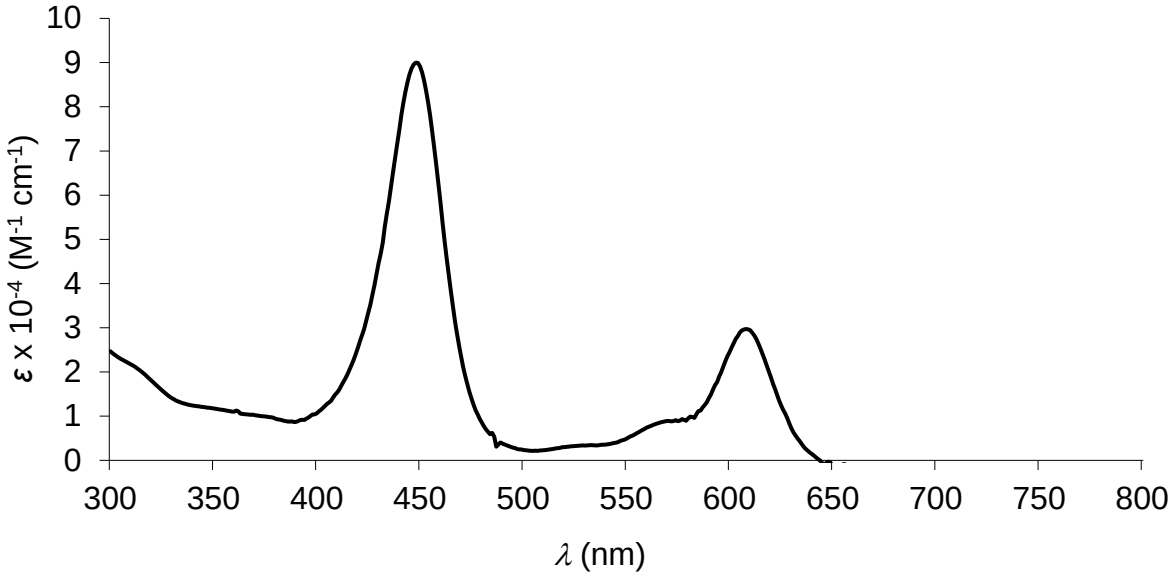

Figure S4. UV-vis spectrum of Re[T*p*FPC-3-CHO](O) in dichloromethane.

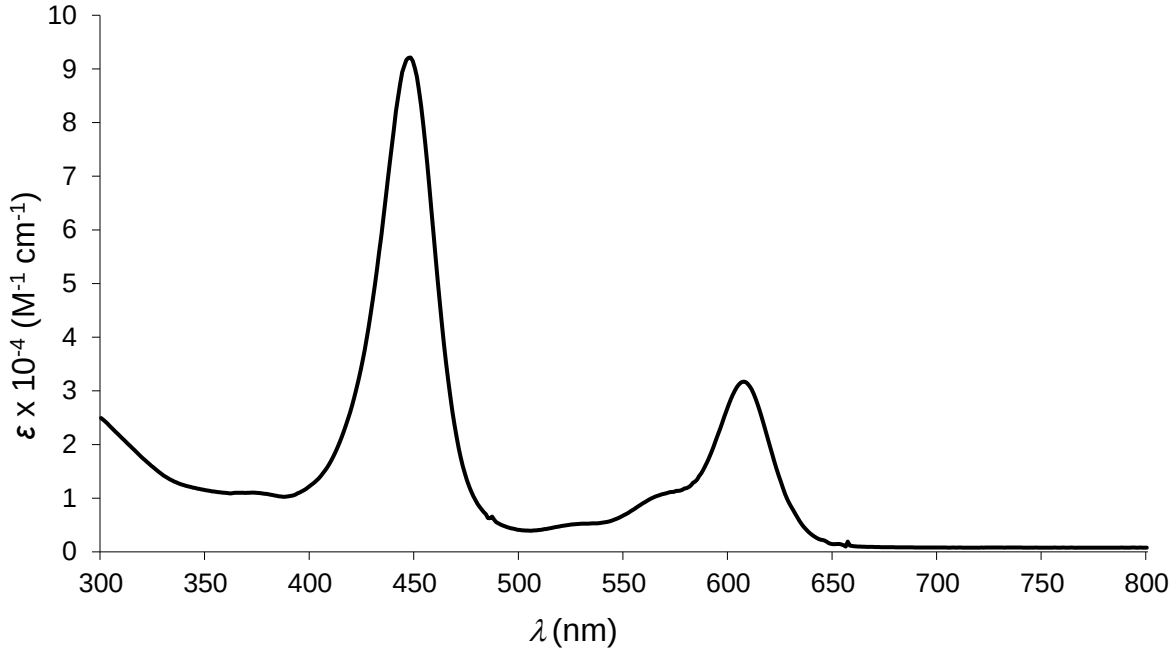

Figure S5. UV-vis spectrum of Re[T*p*CF_3PC-3-CHO](O) in dichloromethane.

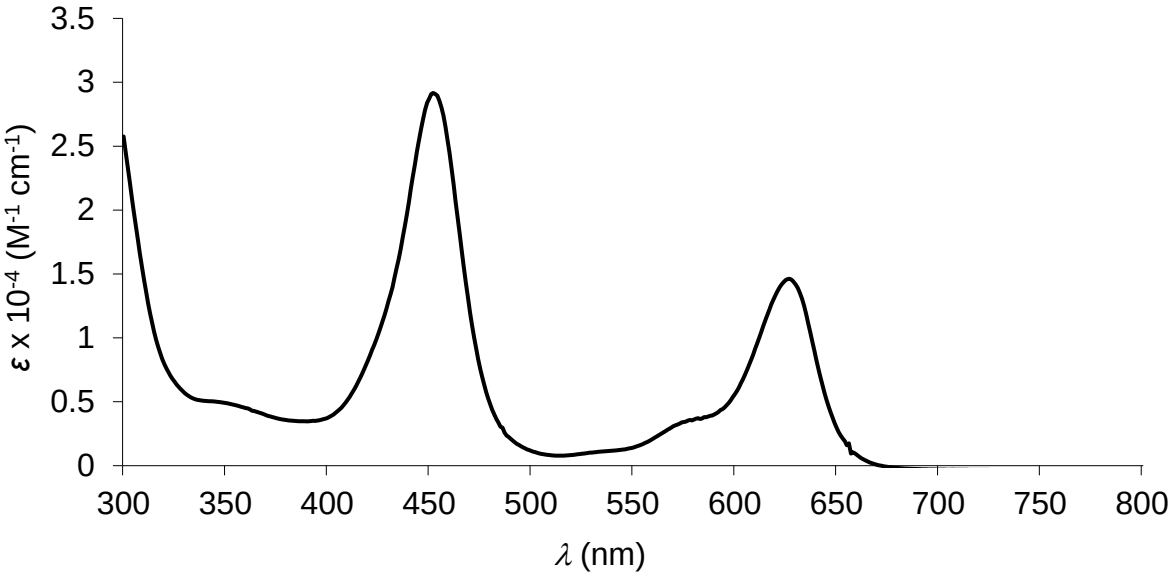

Figure S6. UV-vis spectrum of Re[T*p*FPC-3,17-$(CHO)_2$](O) in dichloromethane.

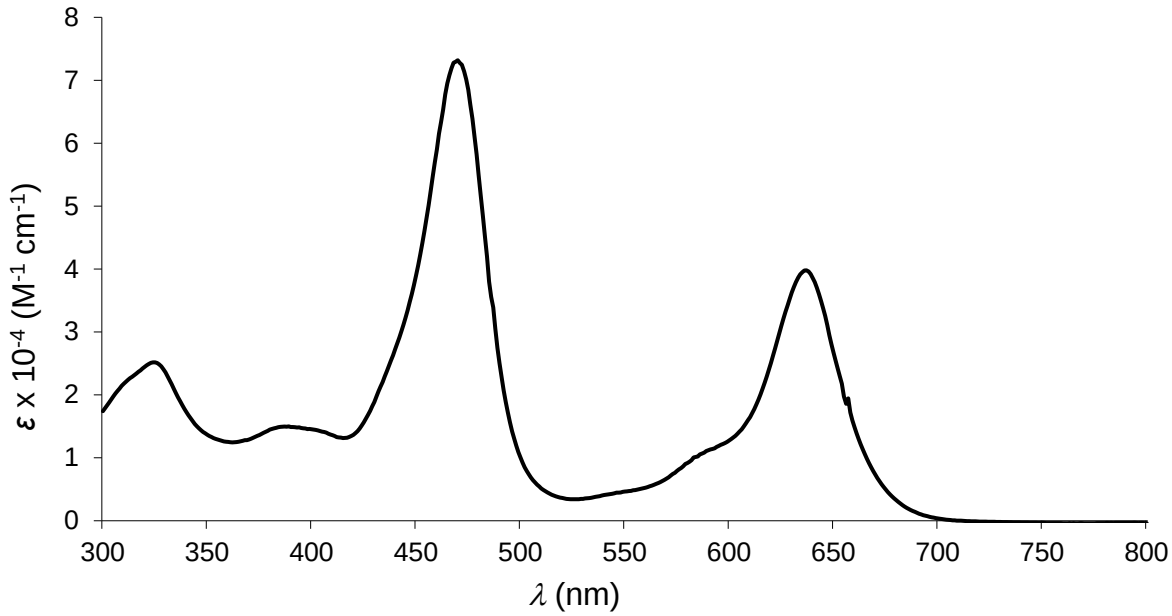

Figure S7. UV-vis spectrum of Re[TPC-3-CH(CN)COOH](O) in dichloromethane.

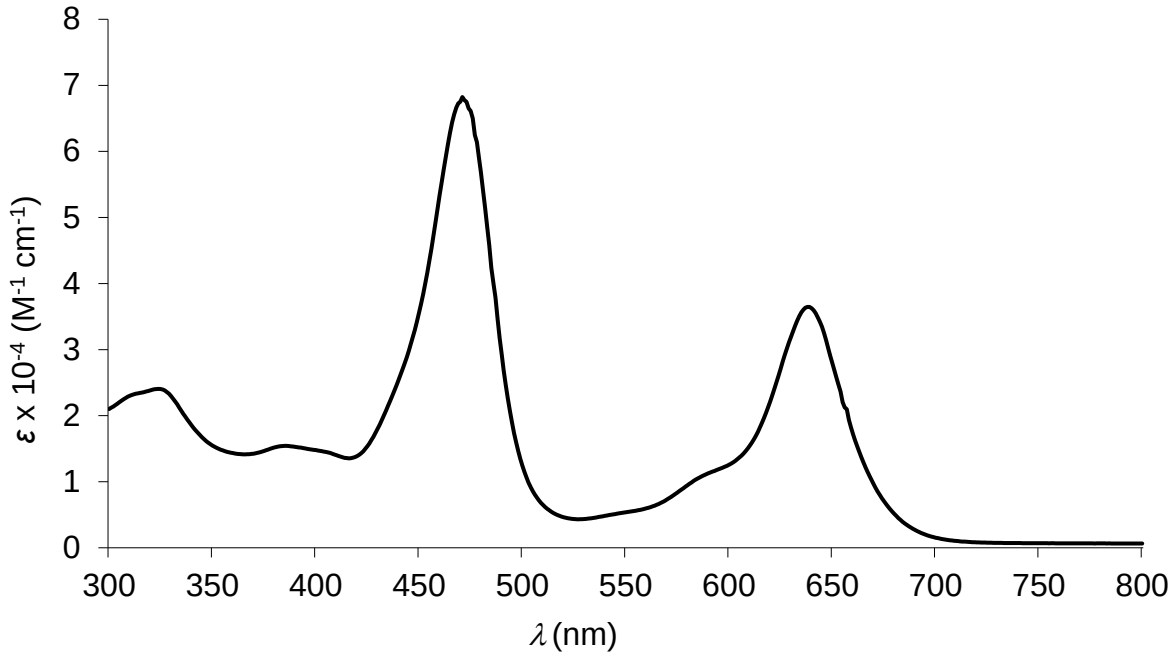

Figure S8. UV-vis spectrum of Re[T*p*CH_3PC-3-CH(CN)COOH](O) in dichloromethane.

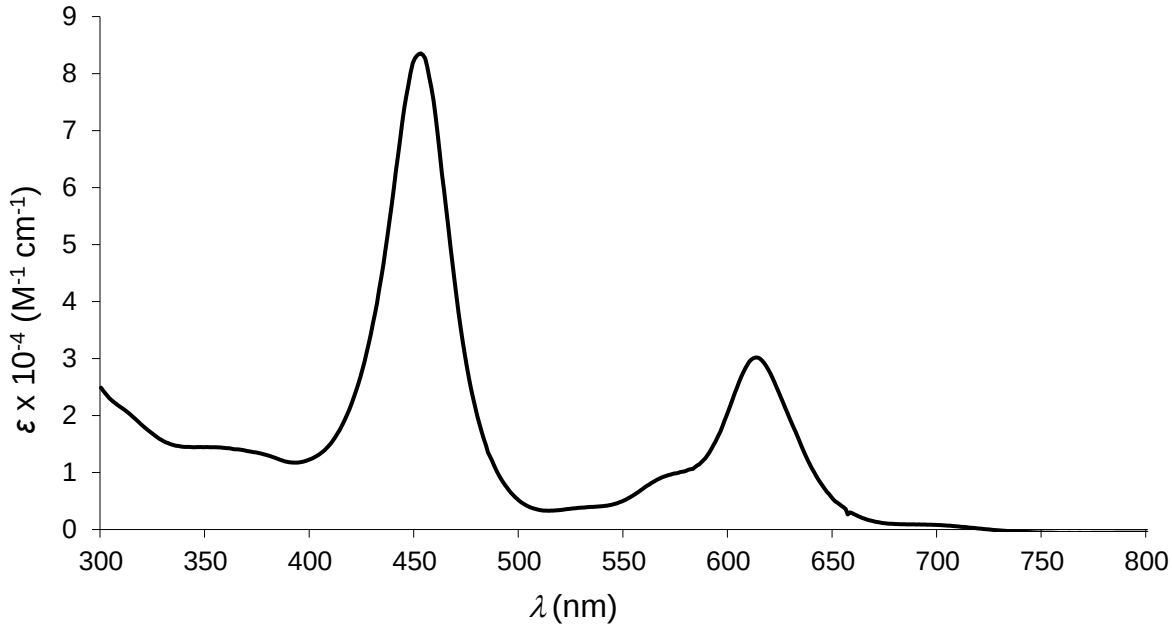

Figure S9. UV-vis spectrum of Re[T*p*OCH$_3$PC-3-CH(CN)COOH](O) in dichloromethane.

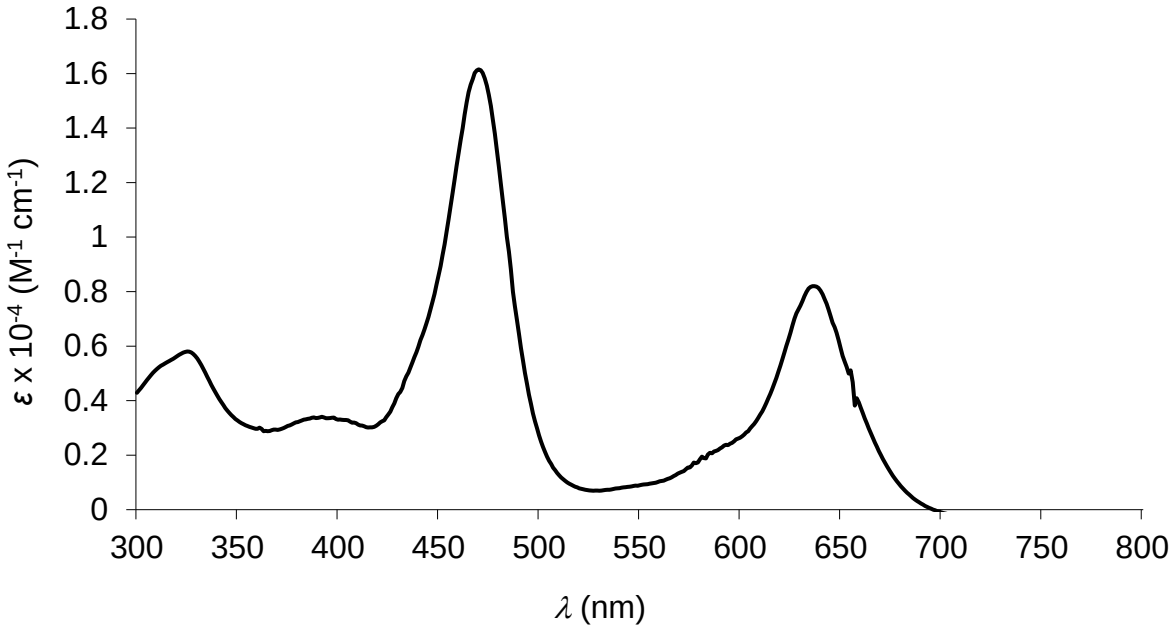

Figure S10. UV-vis spectrum of Re[T*p*FPC-3-CH(CN)COOH](O) in dichloromethane.

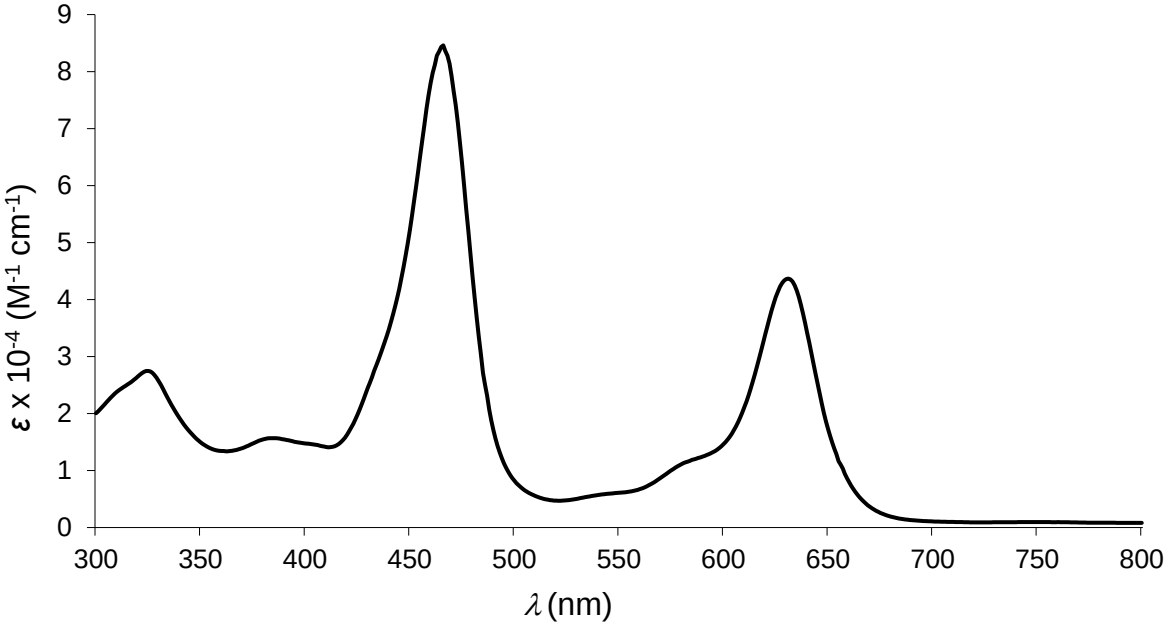

Figure S11. UV-vis spectrum of Re[T*p*CF_3PC-3-CH(CN)COOH](O) in dichloromethane.

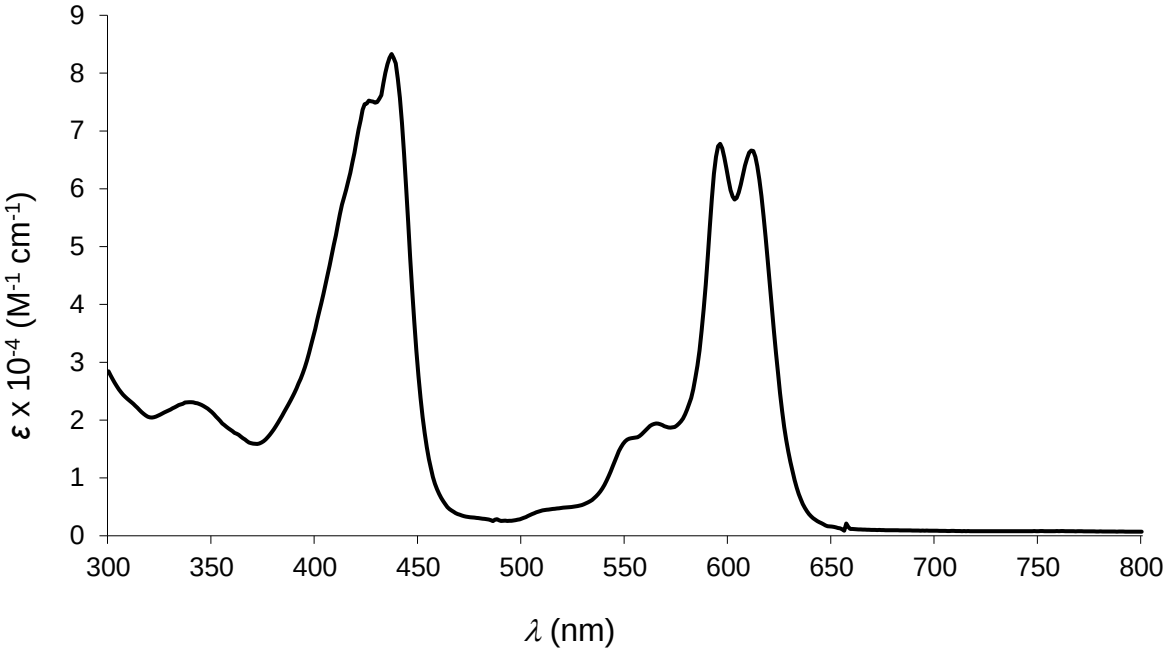

Figure S12. UV-vis spectrum of Au[TPC-3,17-$(CHO)_2$] in dichloromethane.

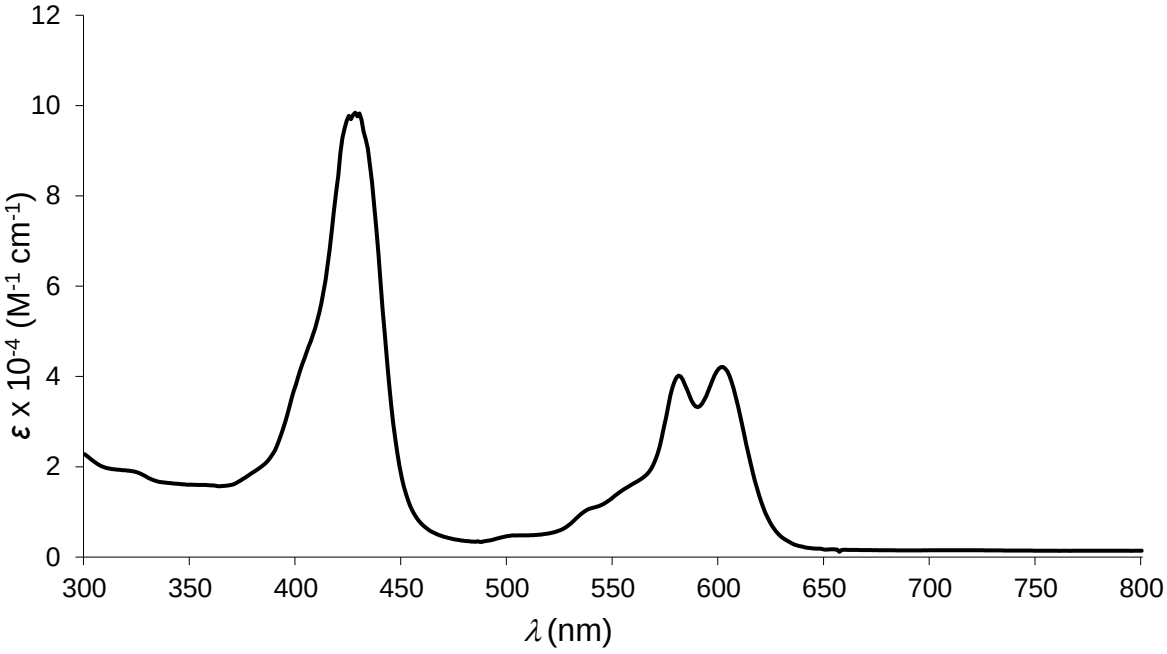

Figure S13. UV-vis spectrum of Au[T*p*CH_3PC-3-CHO] in dichloromethane.

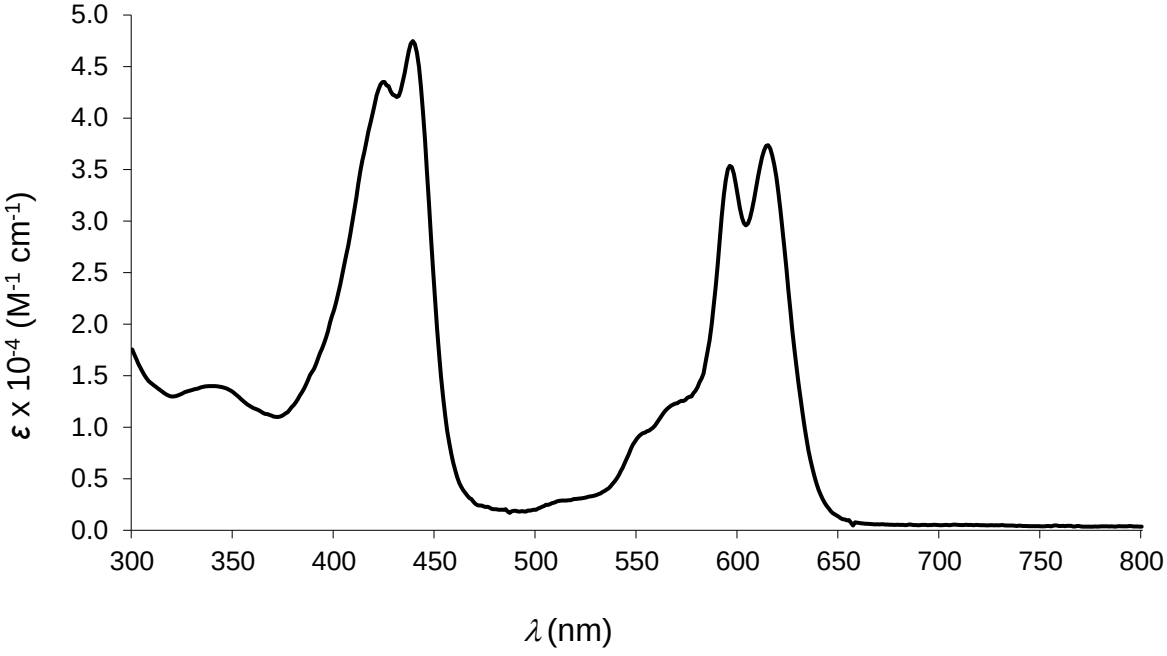

Figure S14. UV-vis spectrum of Au[T*p*CH_3PC-3,17-$(CHO)_2$] in dichloromethane.

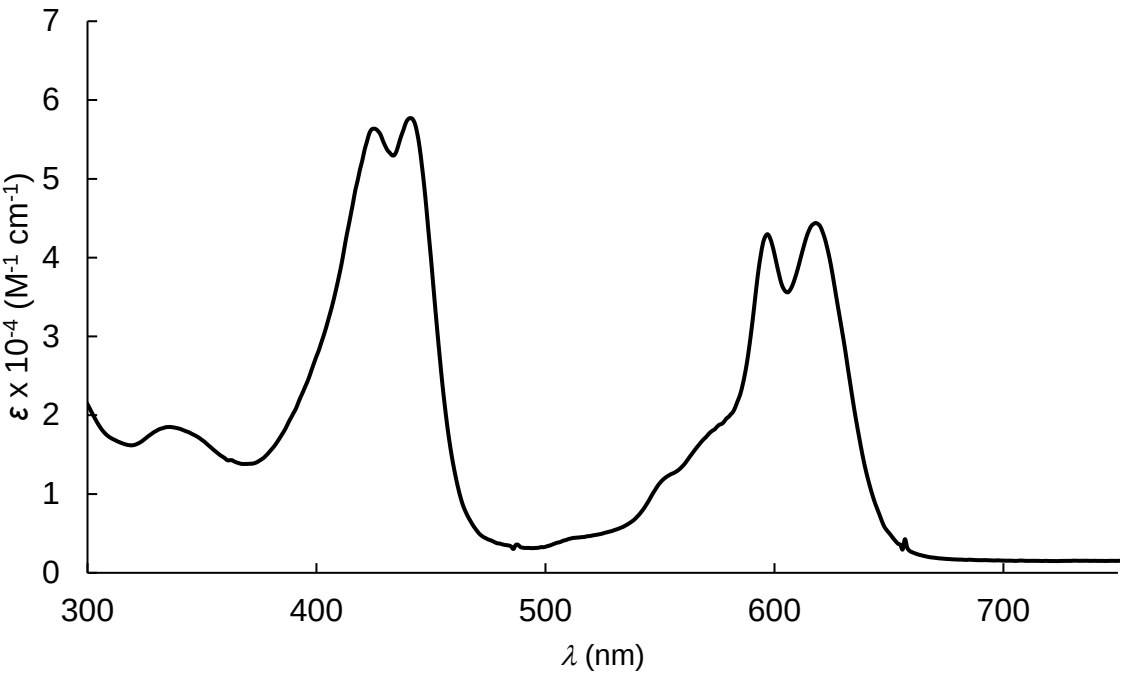

Figure S15. UV-vis spectrum of Au[T*p*OCH$_3$PC-3,17-(CHO)$_2$] in dichloromethane.

B. HRMS-ESI mass spectra

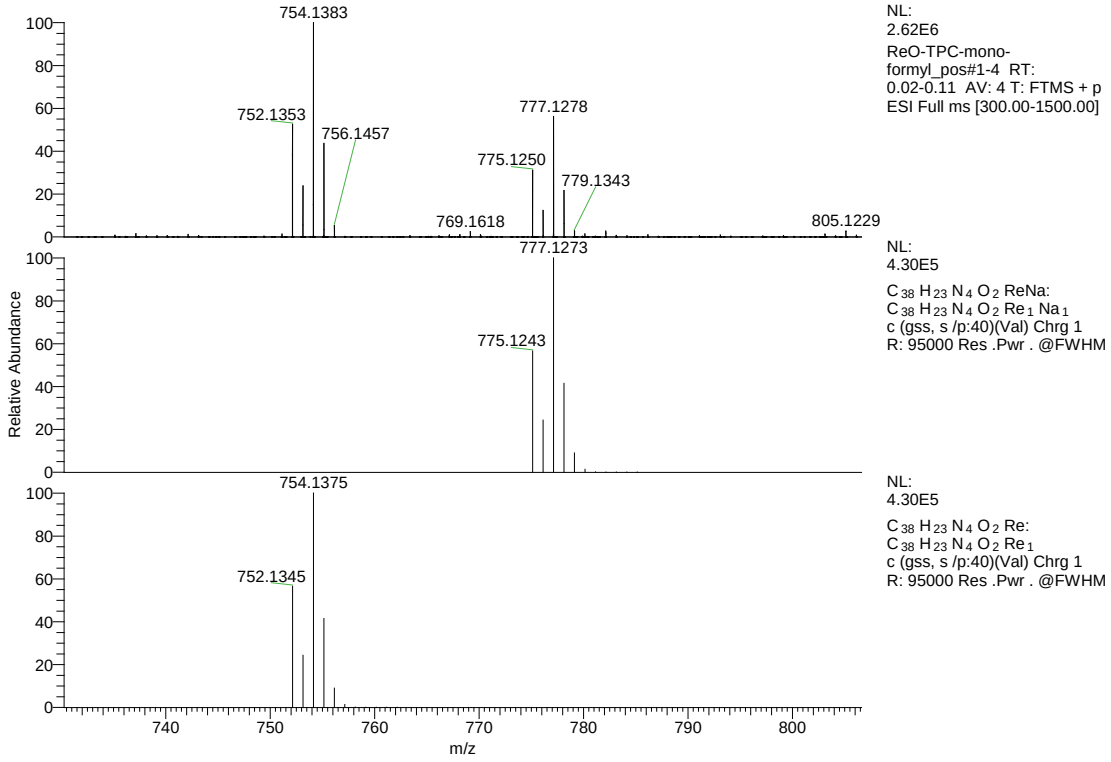

Figure S16. HRMS-ESI mass spectrum of Re[TPC-3-CHO](O).

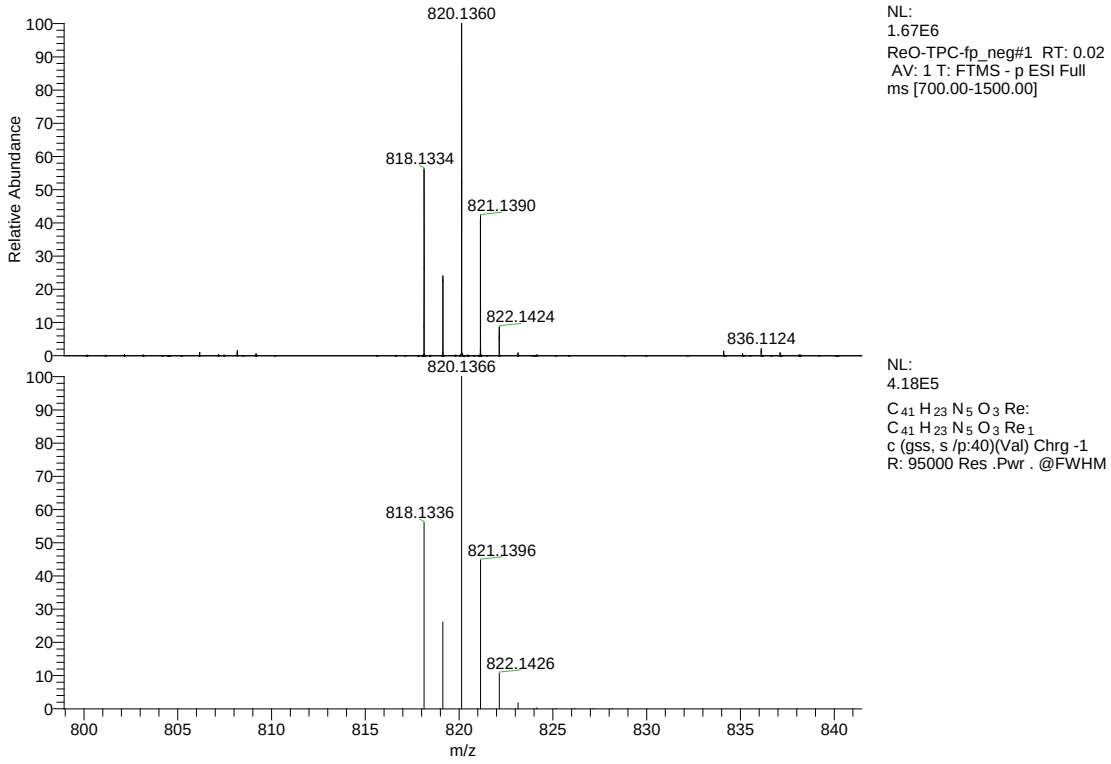

Figure S17. HRMS-ESI mass spectrum of Re[TPC-3-CH(CN)COOH](O).

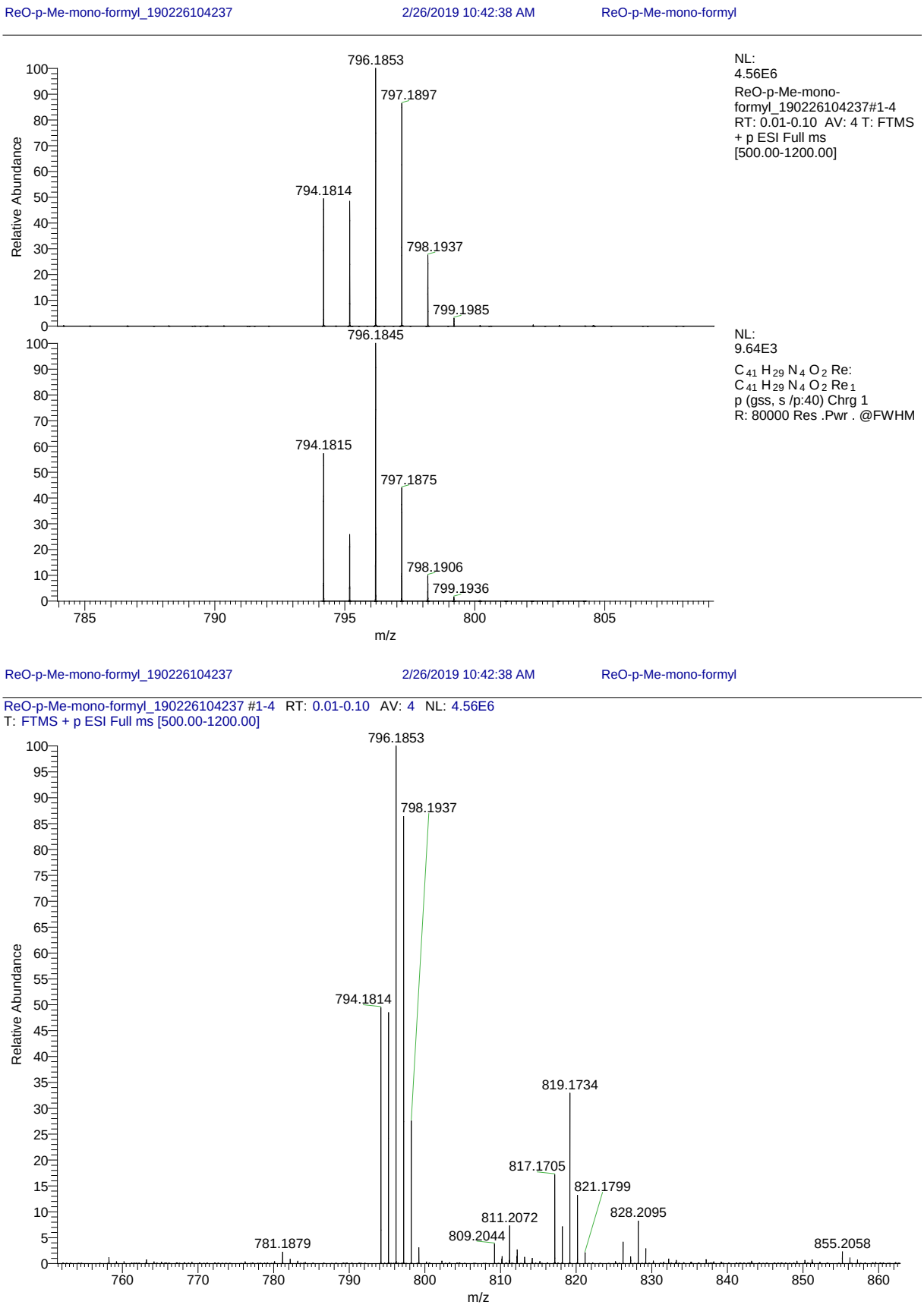

Figure S18. HRMS-ESI mass spectra of Re[T*p*CH$_3$PC-3-CHO](O).

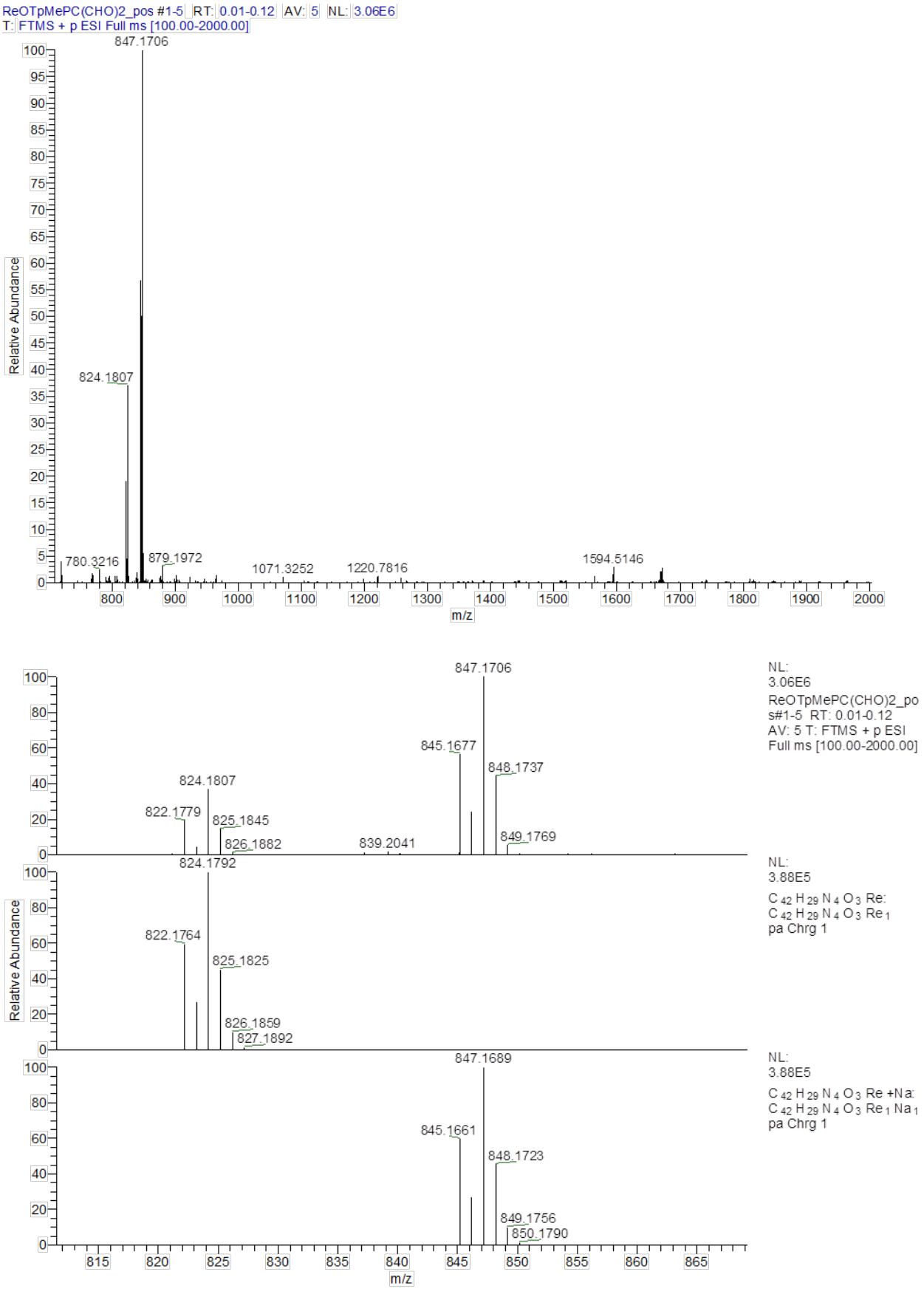

Figure S19. HRMS-ESI mass spectra of Re[T*p*CH$_3$PC-3,17-(CHO)$_2$](O).

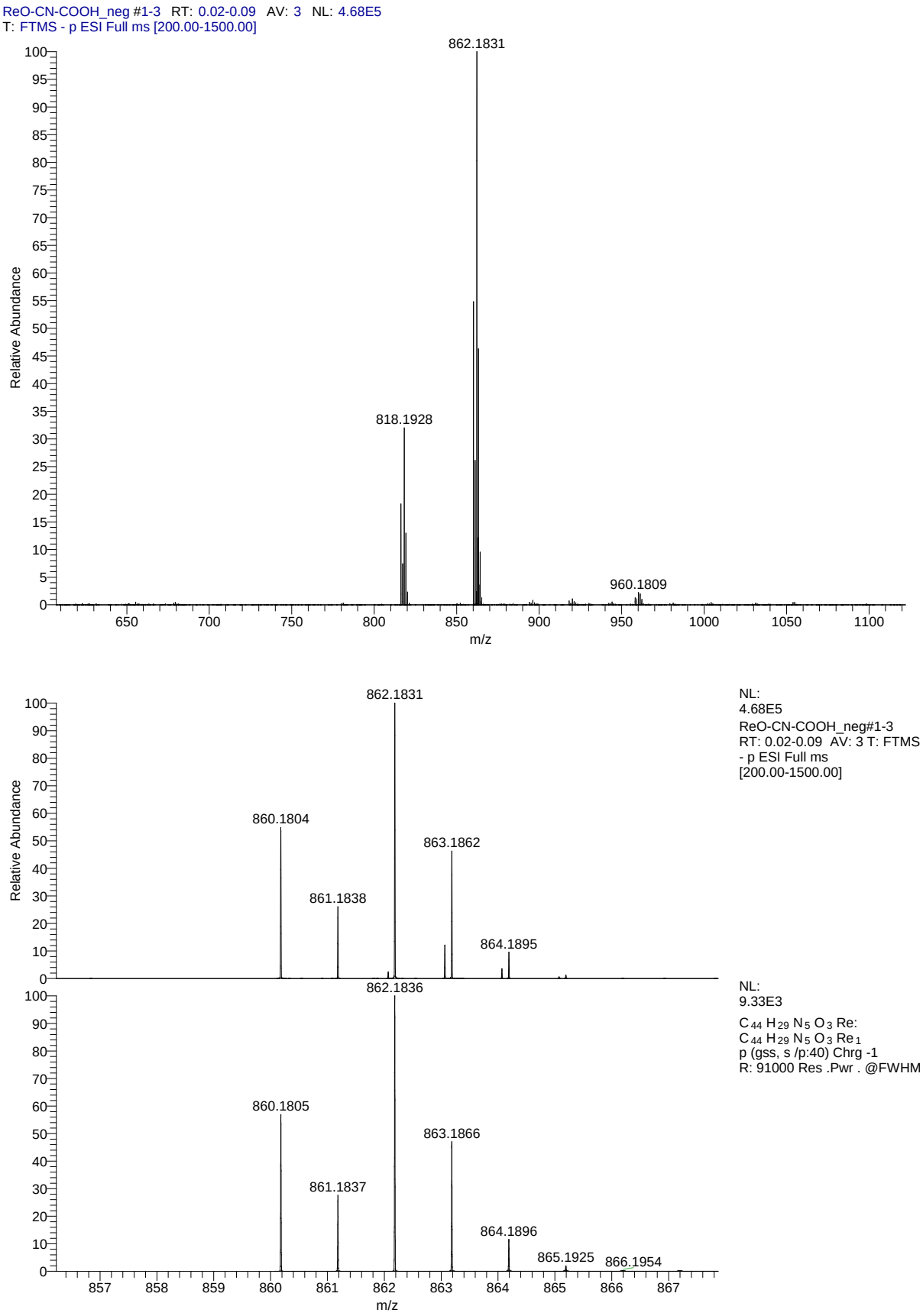

Figure S20. HRMS-ESI mass spectra of Re[T*p*CH$_3$PC-3-CH(CN)COOH](O).

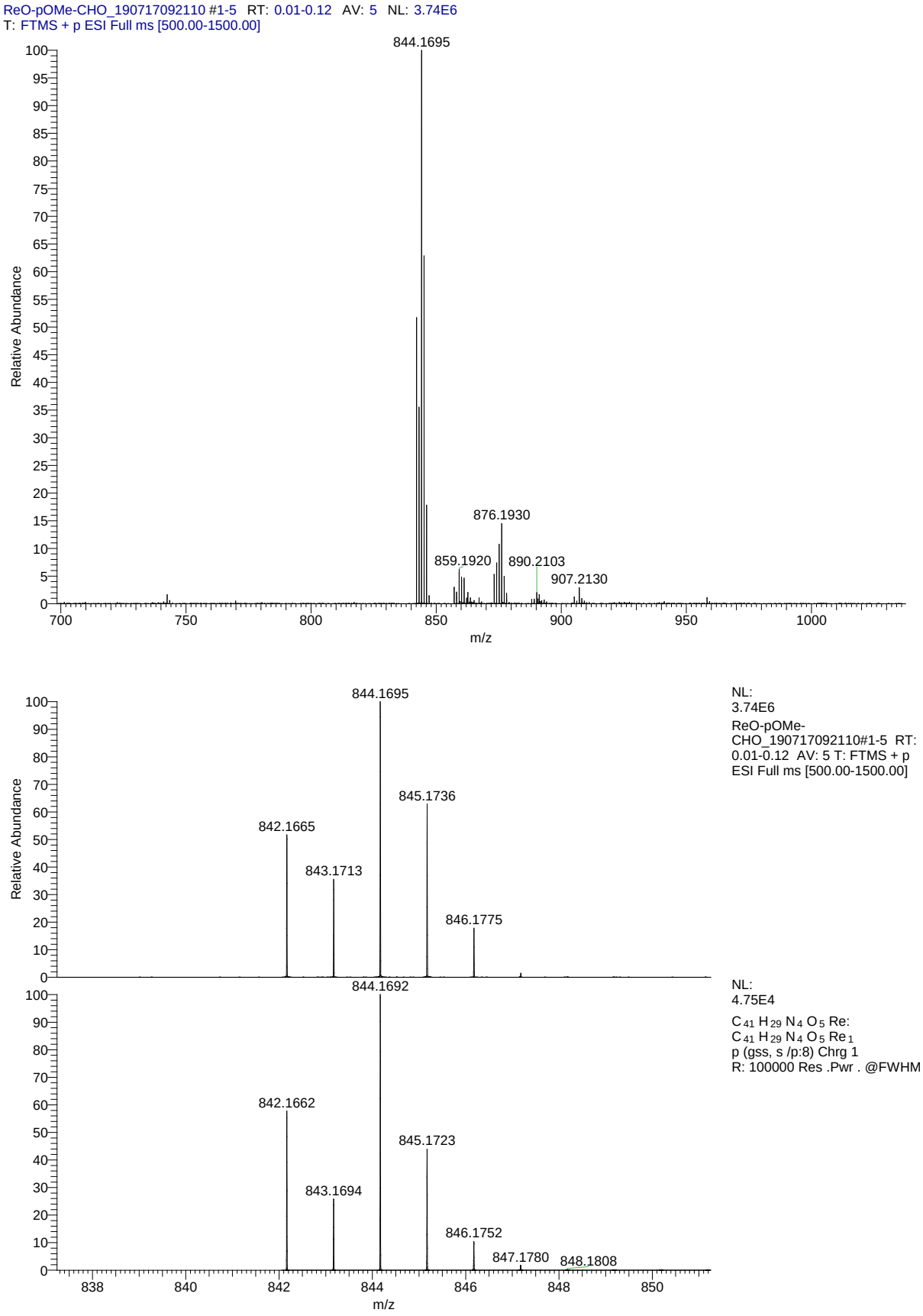

Figure S21. HRMS-ESI mass spectra of Re[T*p*OCH$_3$PC-3-CHO](O).

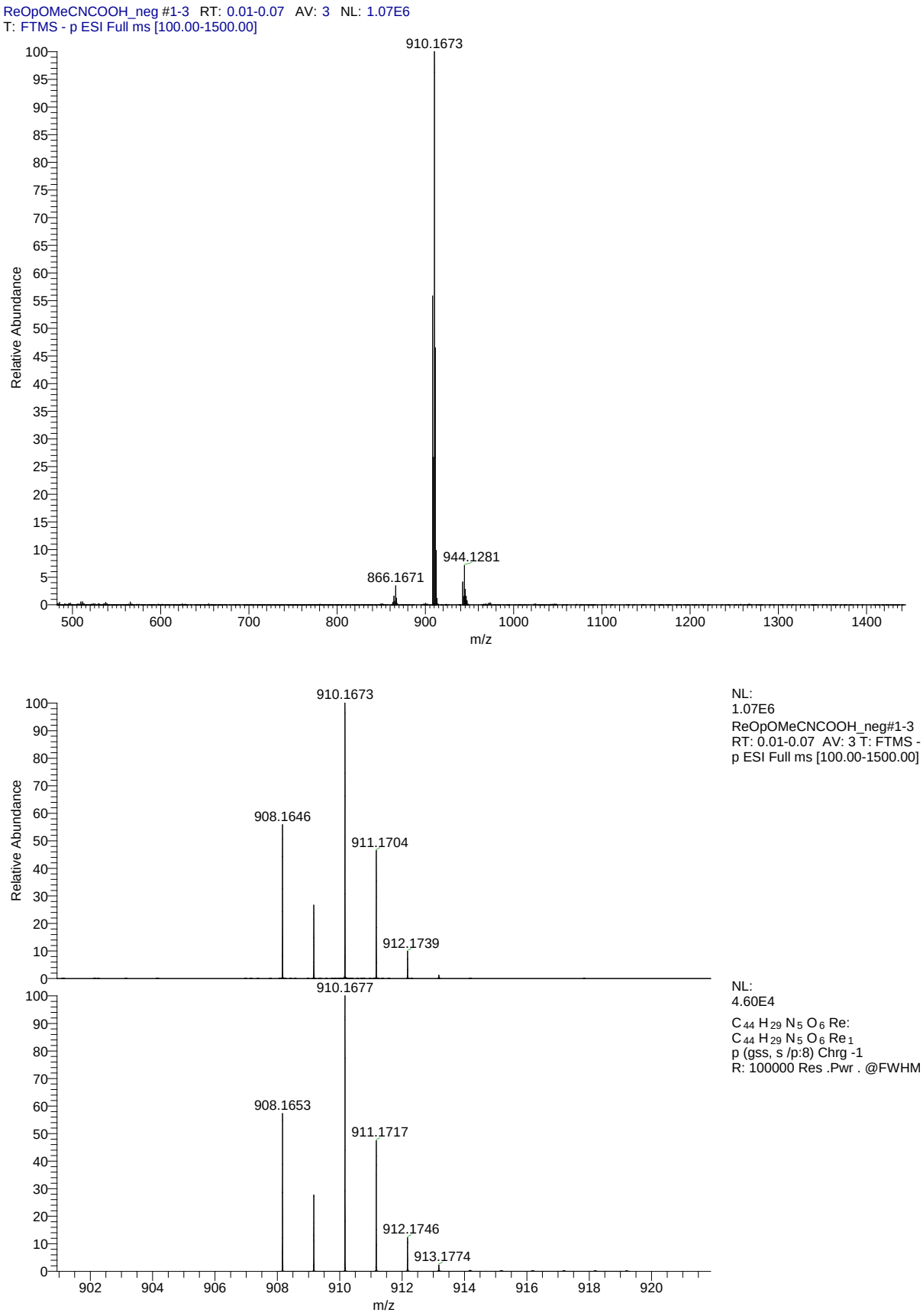

Figure S22. HRMS-ESI mass spectra of Re[T*p*OCH$_3$PC-3-CH(CN)COOH](O).

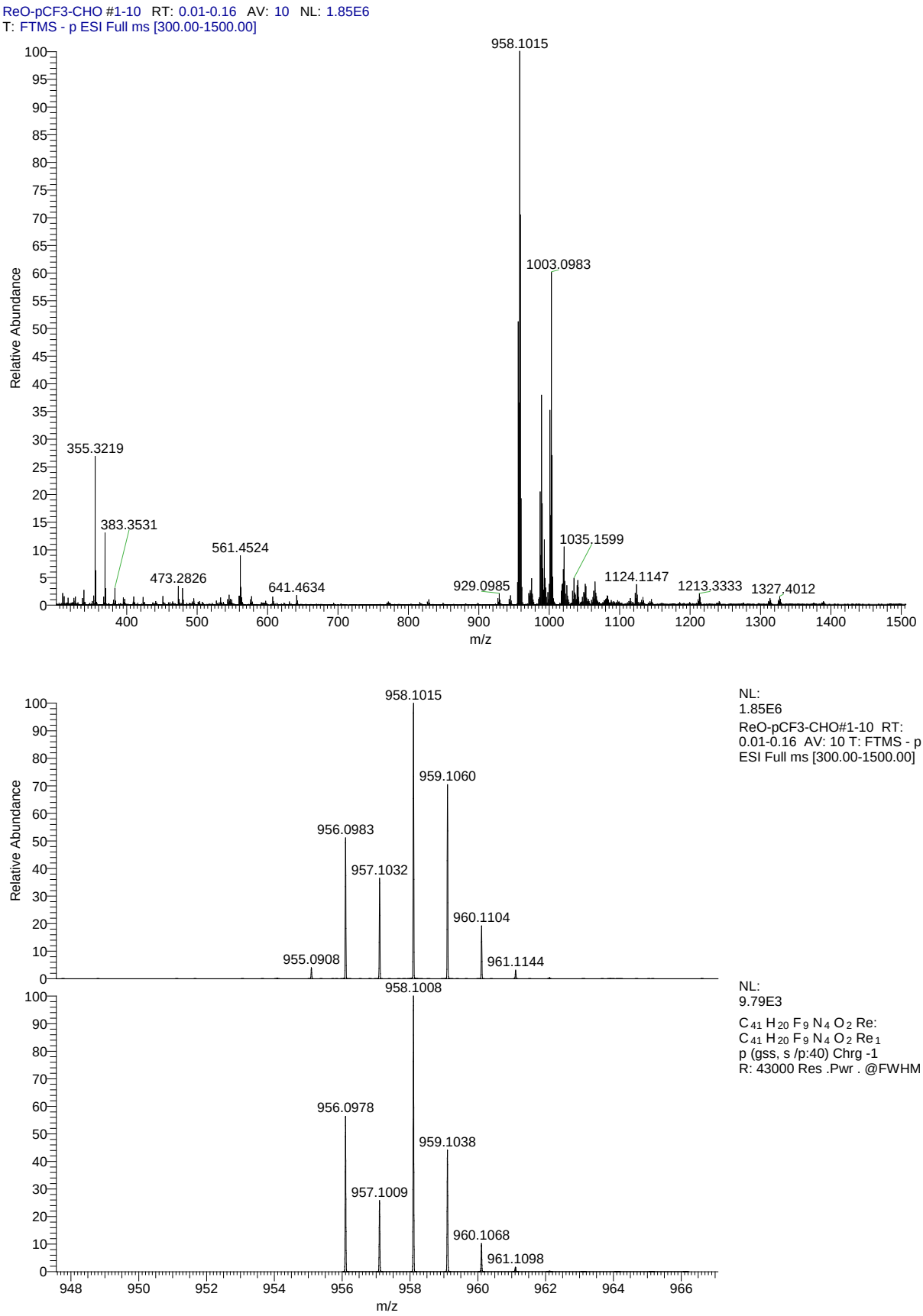

Figure S23. HRMS-ESI mass spectra of Re[T*p*CF_3PC-3-CHO](O).

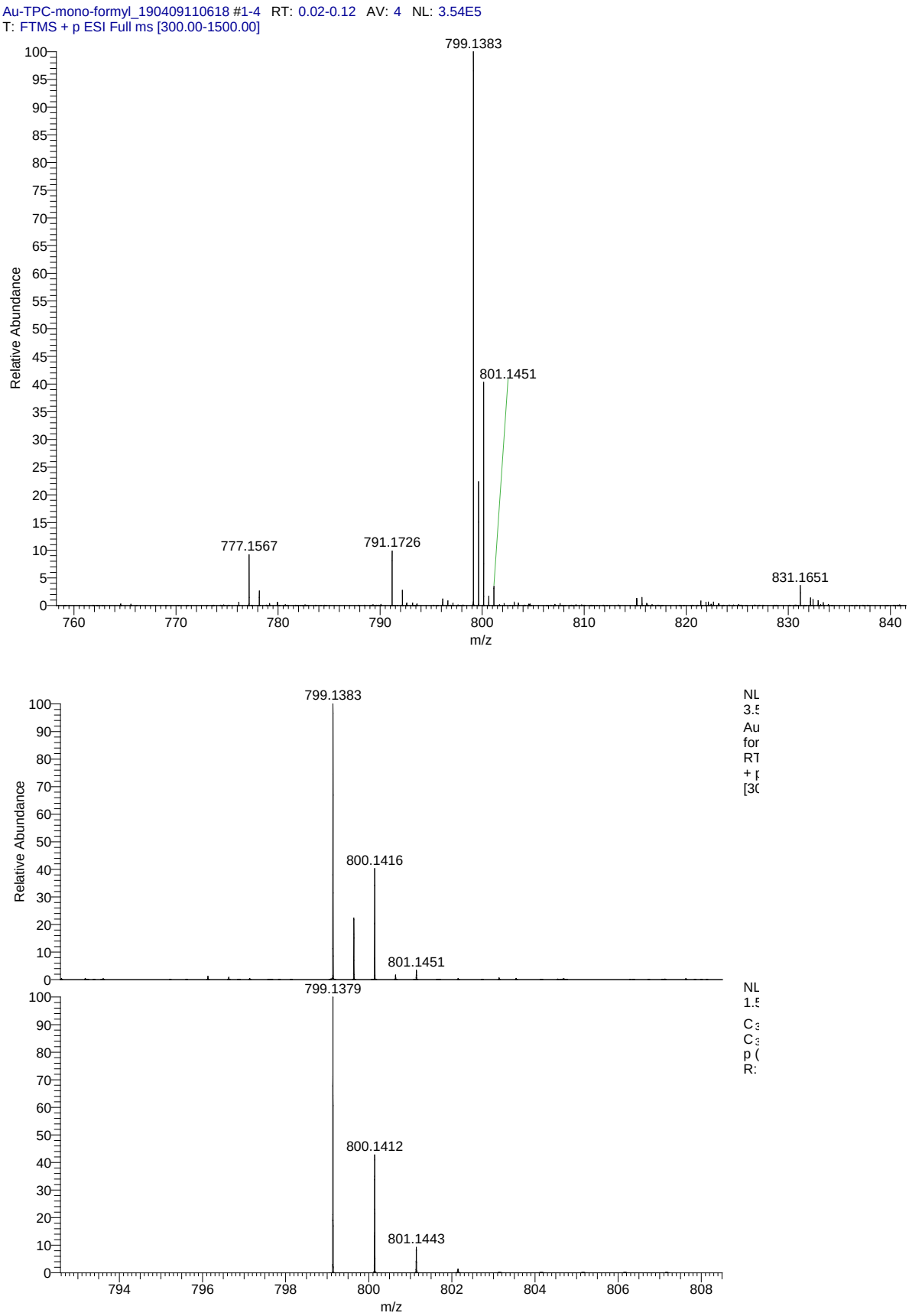

Figure S24. HRMS-ESI mass spectrum of Au[TPC-3,17-(CHO)$_2$].

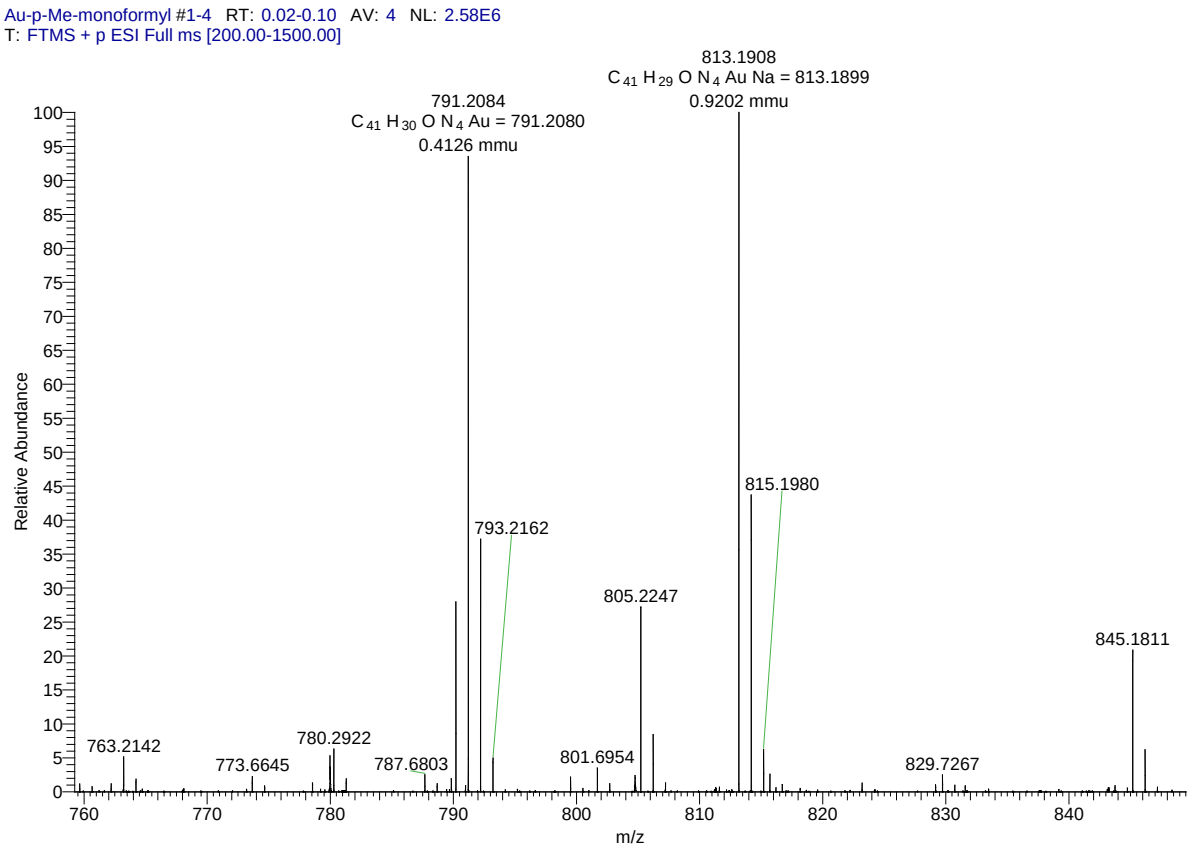

Figure S25. HRMS-ESI mass spectrum of Au[T*p*CH_3PC-3-CHO].

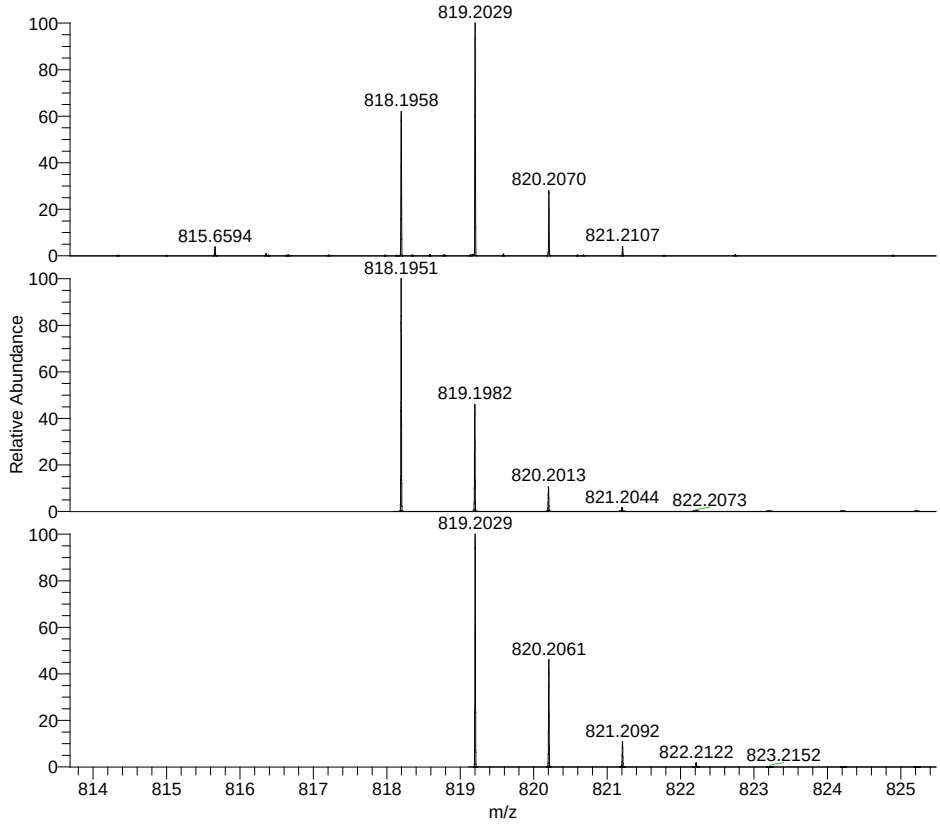

Figure S26. HRMS-ESI mass spectrum of Au[T*p*CH_3PC-3,17-$(CHO)_2$].

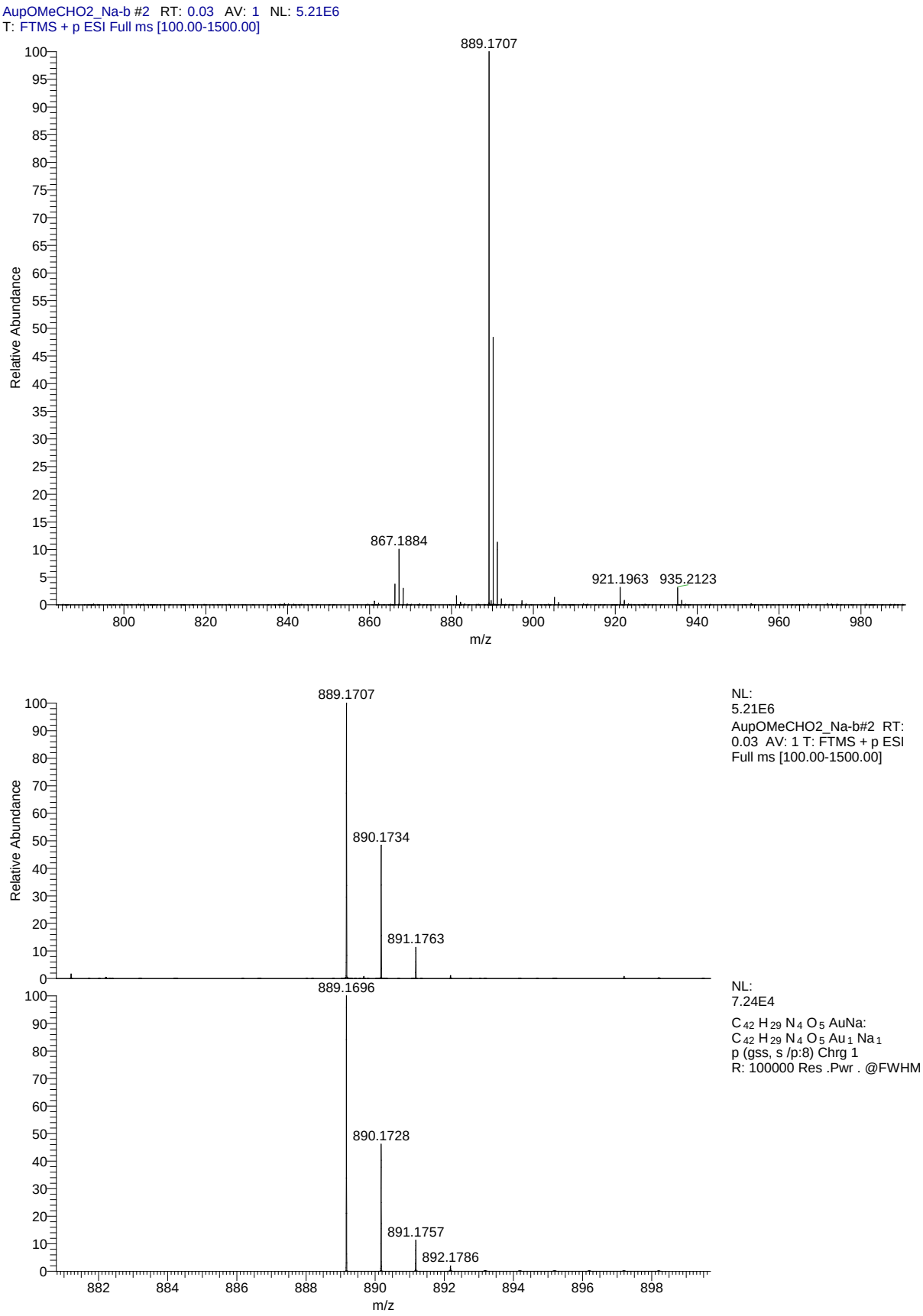

Figure S27. HRMS-ESI mass spectrum of Au[T*p*OCH$_3$PC-3,17-(CHO)$_2$].

C. ^{1}H NMR spectra

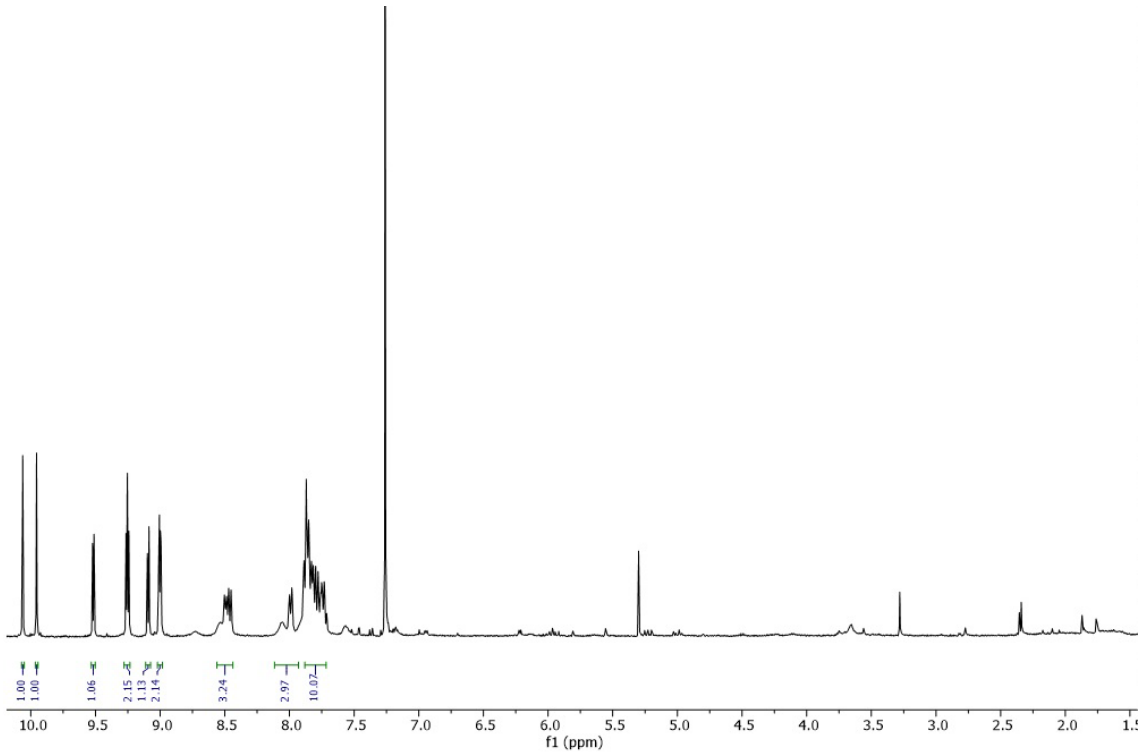

Figure S28. ^{1}H NMR spectrum of Re[TPC-3-CHO](O) at -20°C.

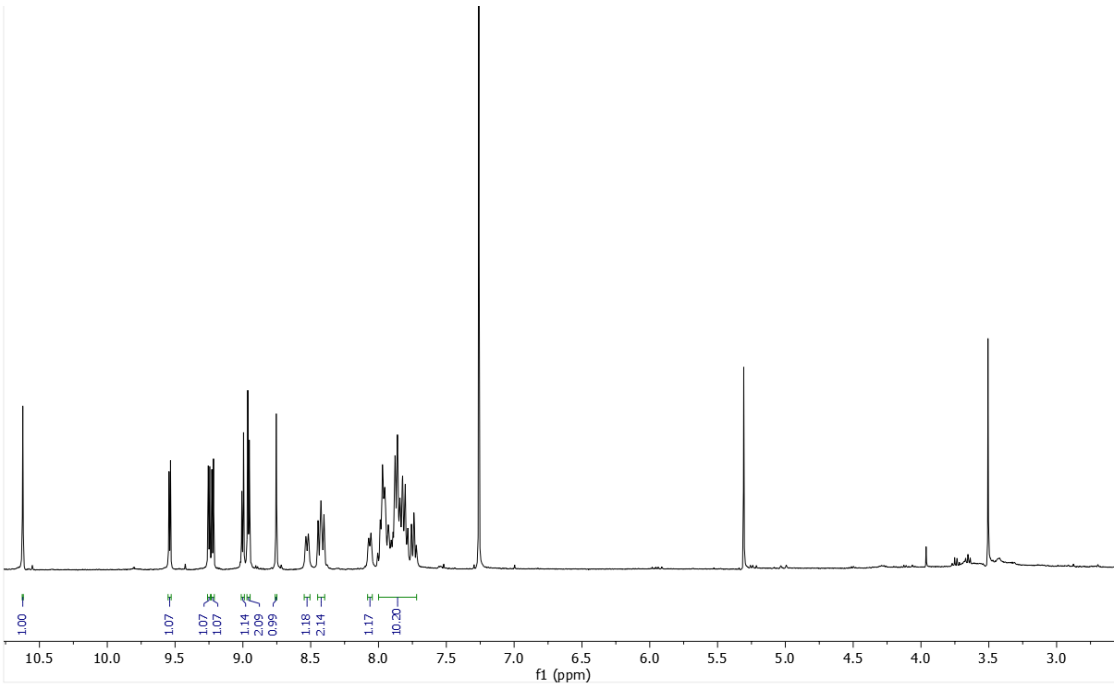

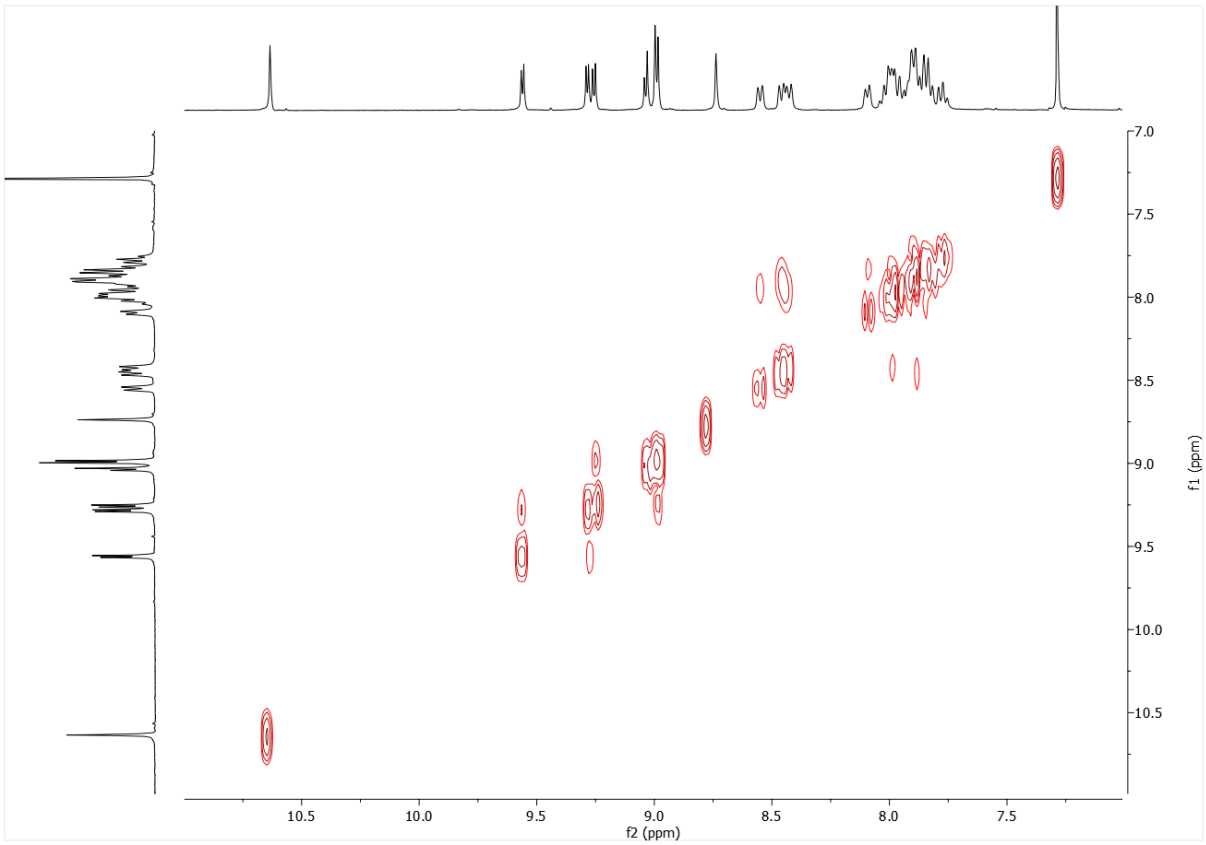

Figure S29. ^{1}H NMR and ^{1}H—^{1}H COSY spectra of Re[TPC-3-CH(CN)COOH](O) at -20°C.

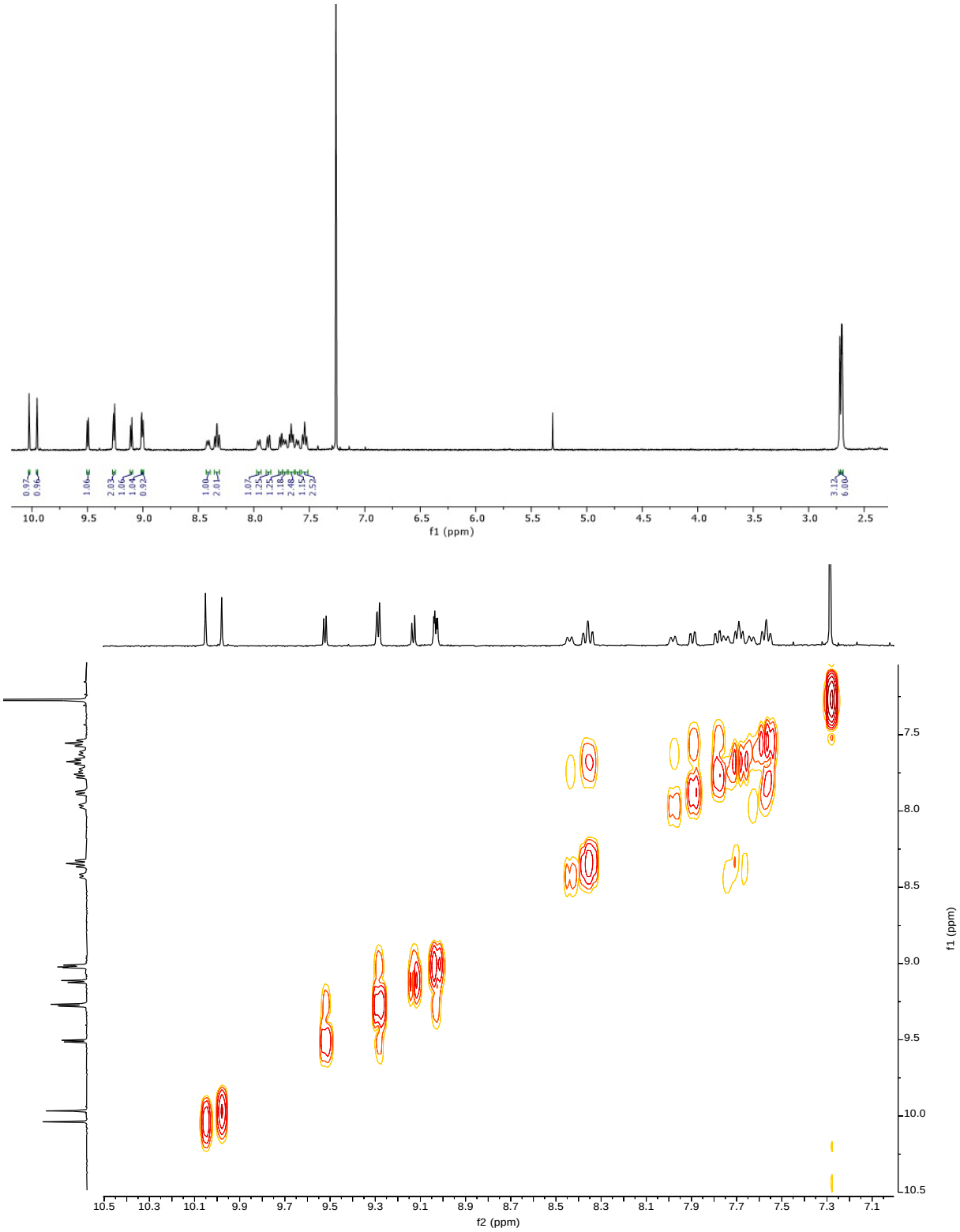

Figure S30. ^{1}H NMR and ^{1}H—^{1}H COSY spectrum of Re[T*p*CH$_3$PC-3-CHO](O) at -20°C.

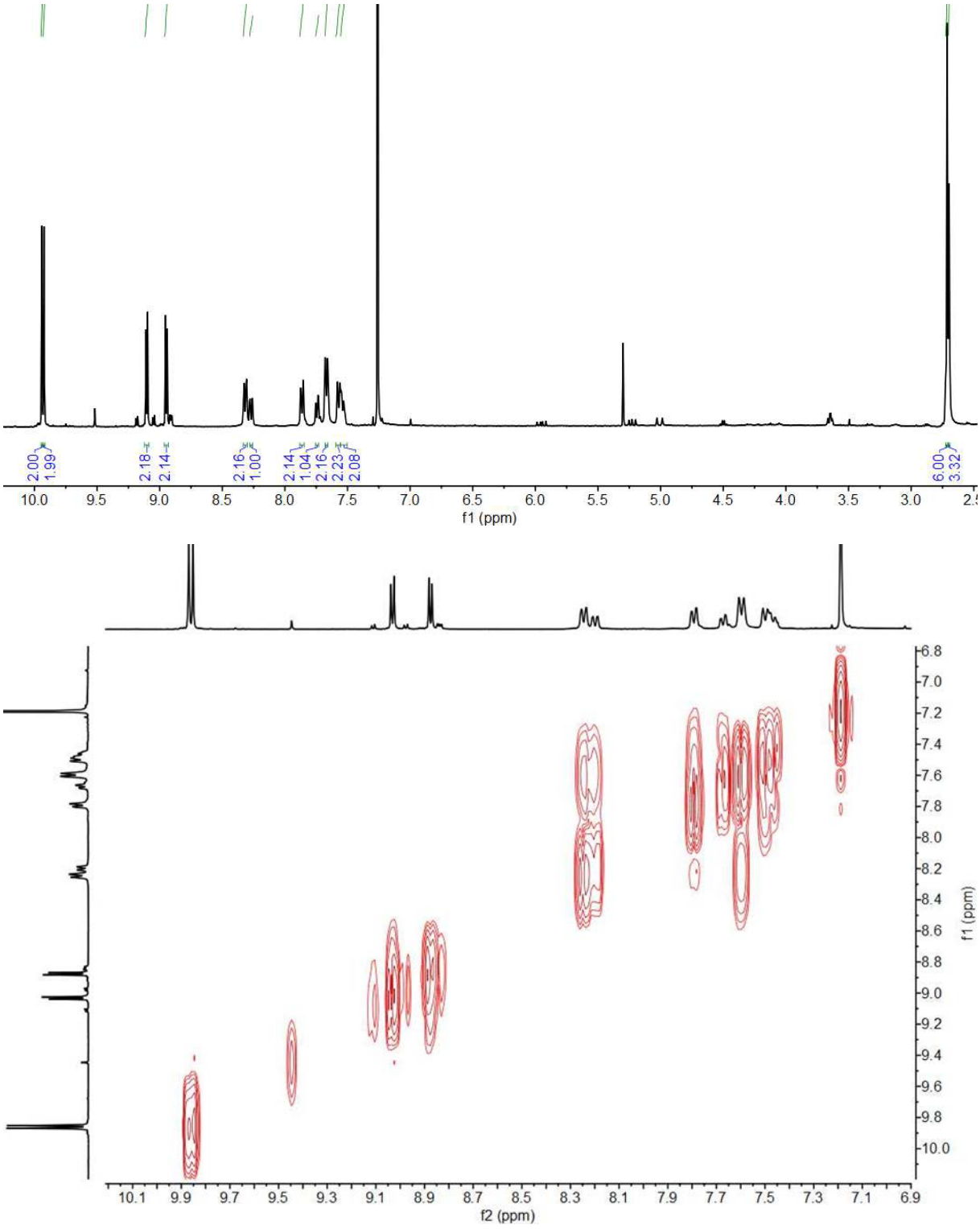

Figure S31. ^{1}H NMR and ^{1}H—^{1}H COSY spectra of Re[T*p*CH$_3$PC-3,17-(CHO)$_2$](O) at -20°C.

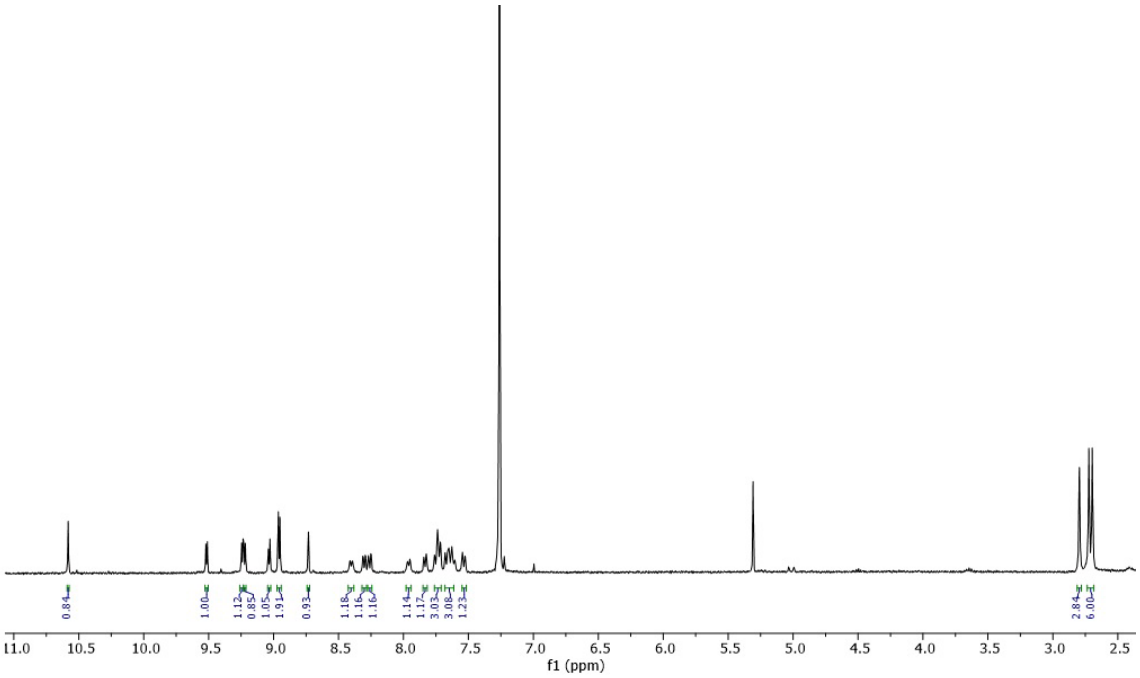

Figure S32. ^{1}H NMR spectrum of Re[T*p*CH_3PC-3-CH(CN)COOH](O) in $CDCl_3$ at -20°C.

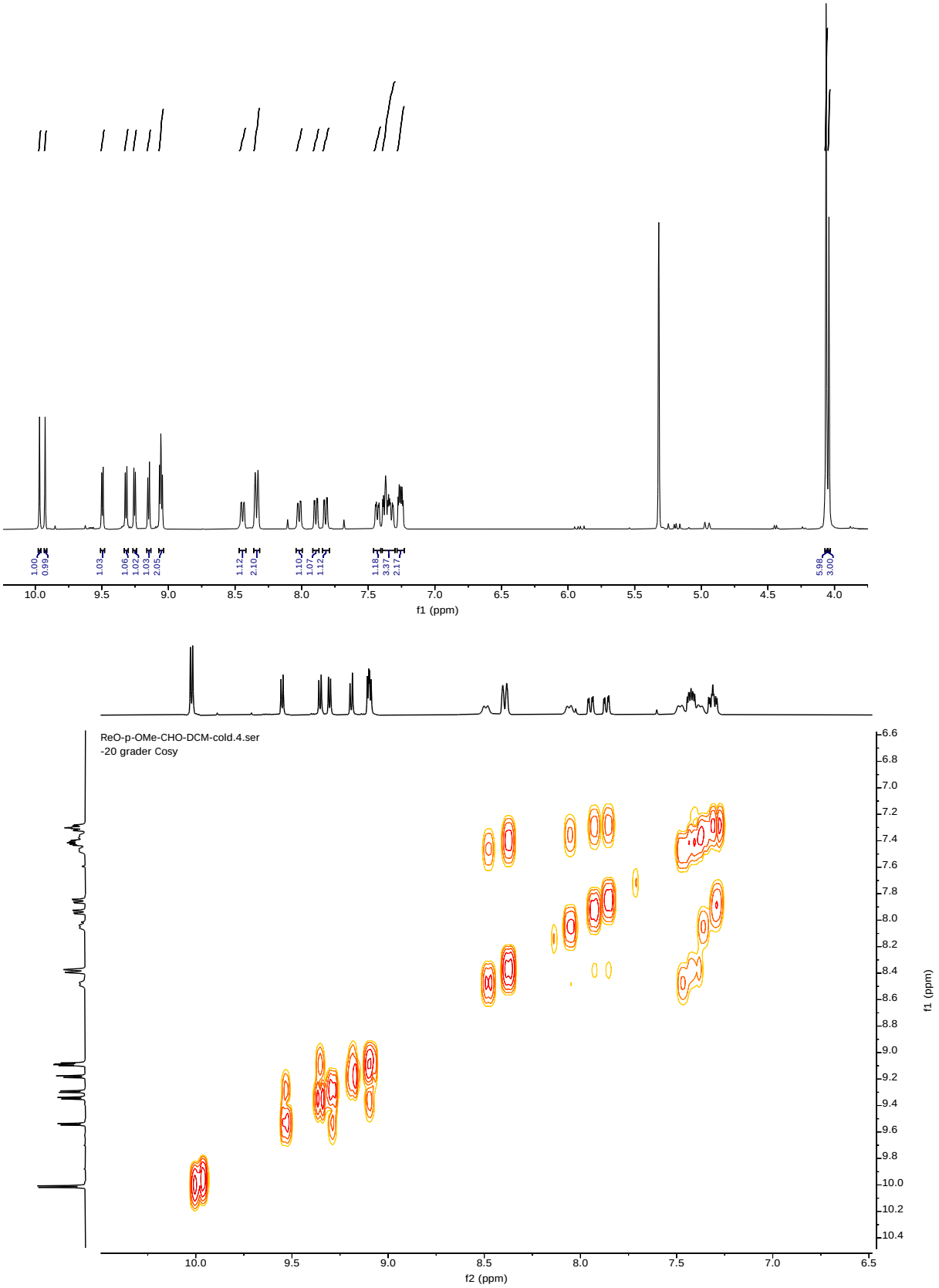

Figure S33. ^{1}H NMR and ^{1}H—^{1}H COSY spectra of Re[T*p*OCH$_3$PC-3-CHO](O) in CDCl$_3$ at -20°C.

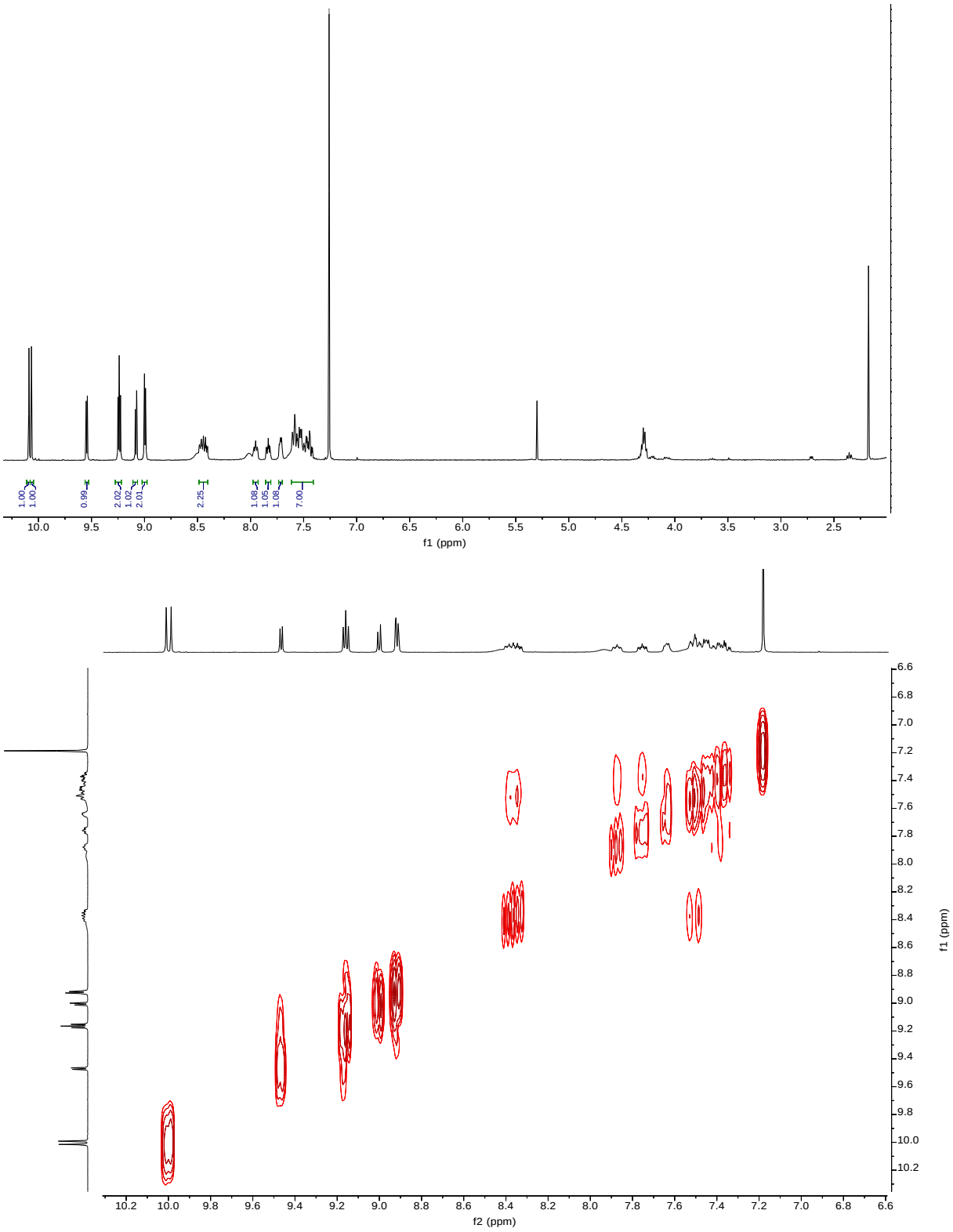

Figure S34. ^{1}H NMR and ^{1}H—^{1}H COSY spectra of Re[T*p*FPC-3-CHO]O in $CDCl_3$ at 20°C.

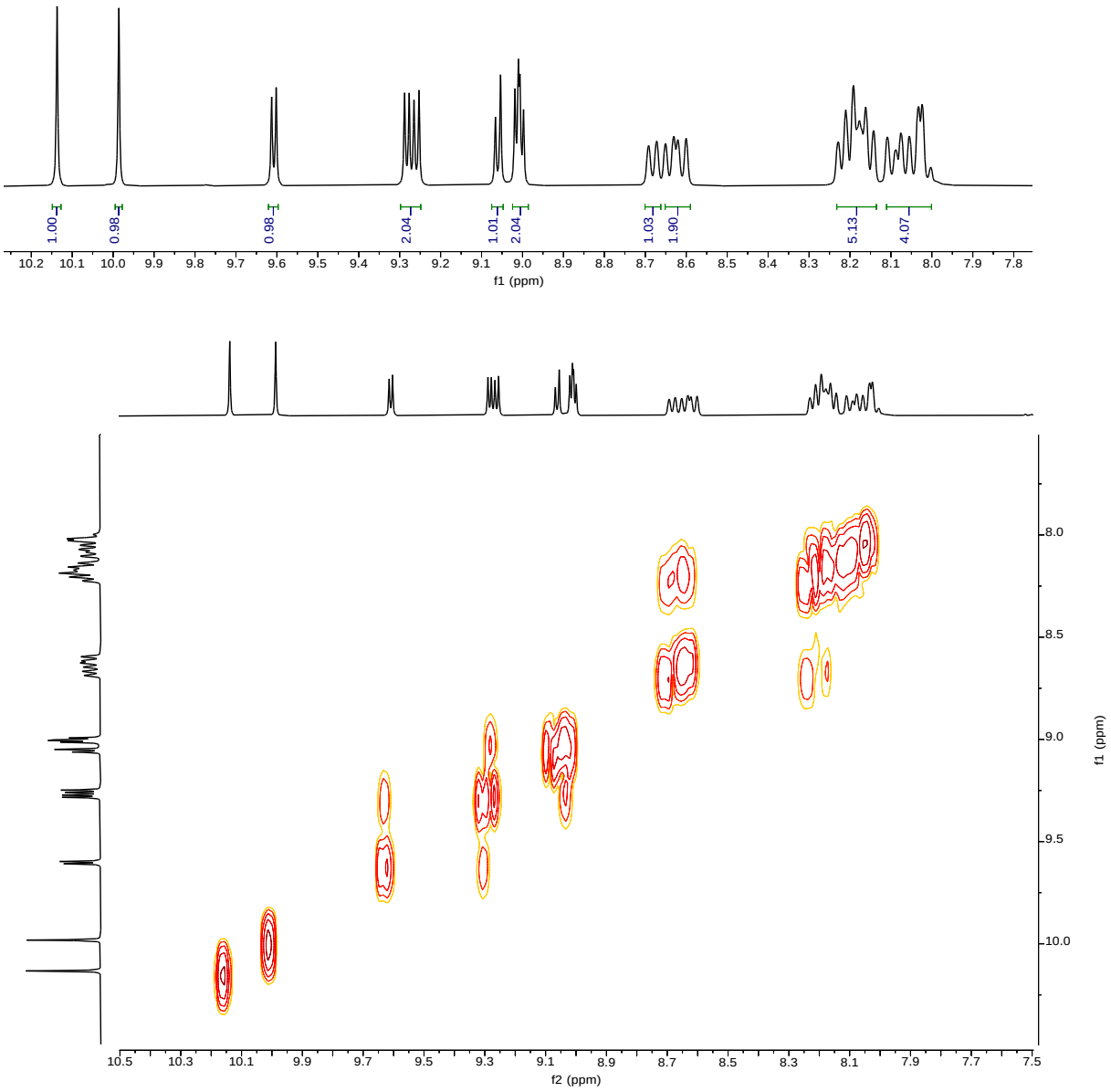

Figure S35. ^{1}H NMR and ^{1}H—^{1}H COSY spectra of Re[T*p*CF$_3$PC-3-CHO]O in CDCl$_3$ at -20°C.

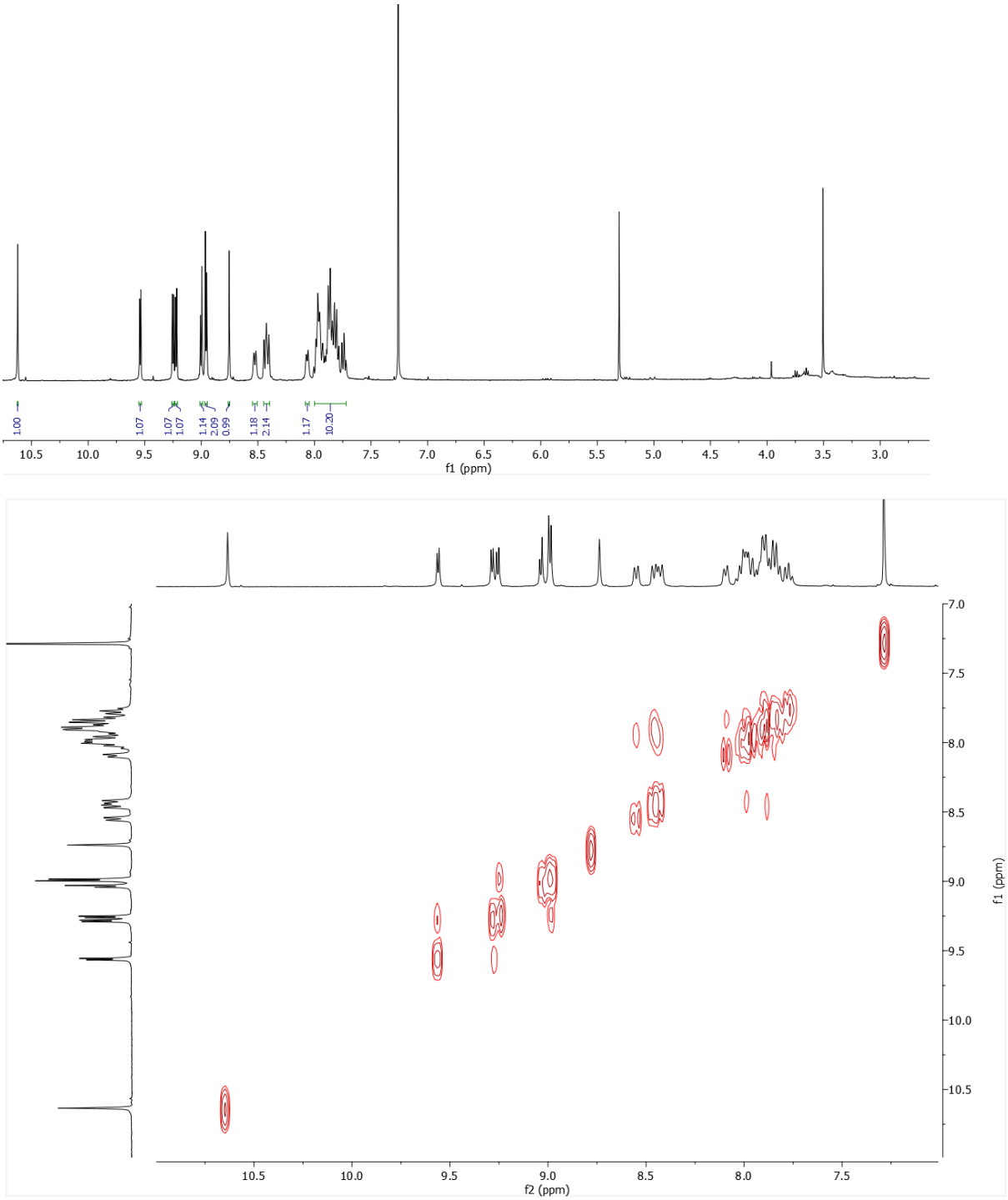

Figure S36. ^{1}H NMR and ^{1}H—^{1}H COSY spectra of Re[TPC-3-CH(CN)COOH](O) in $CDCl_3$ at -20°C.

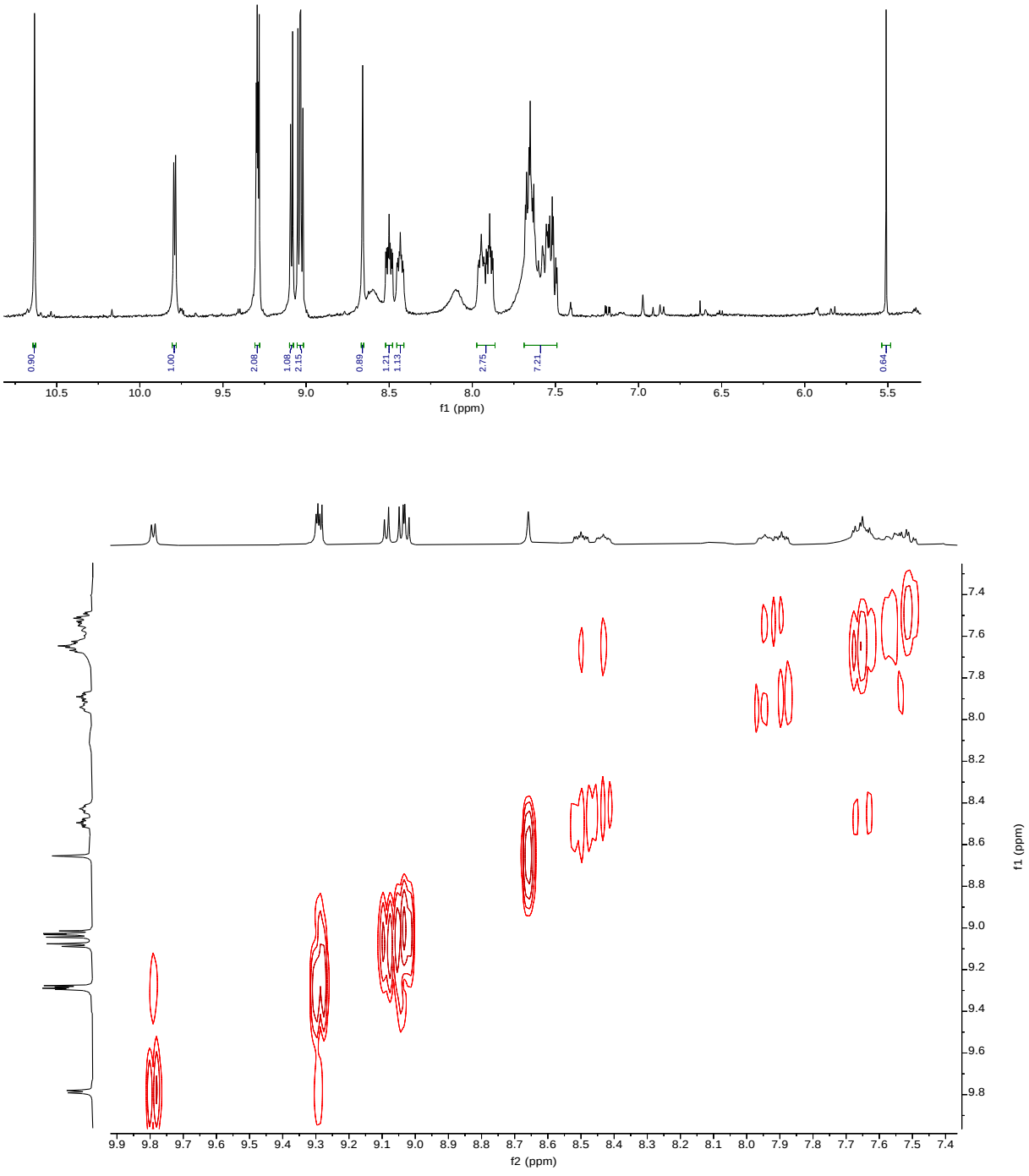

Figure S37. ^{1}H NMR and ^{1}H—^{1}H COSY spectra of Re[T*p*FPC-3-(CN)COOH](O) in tetrahydrofuran-d_8 at 20°C.

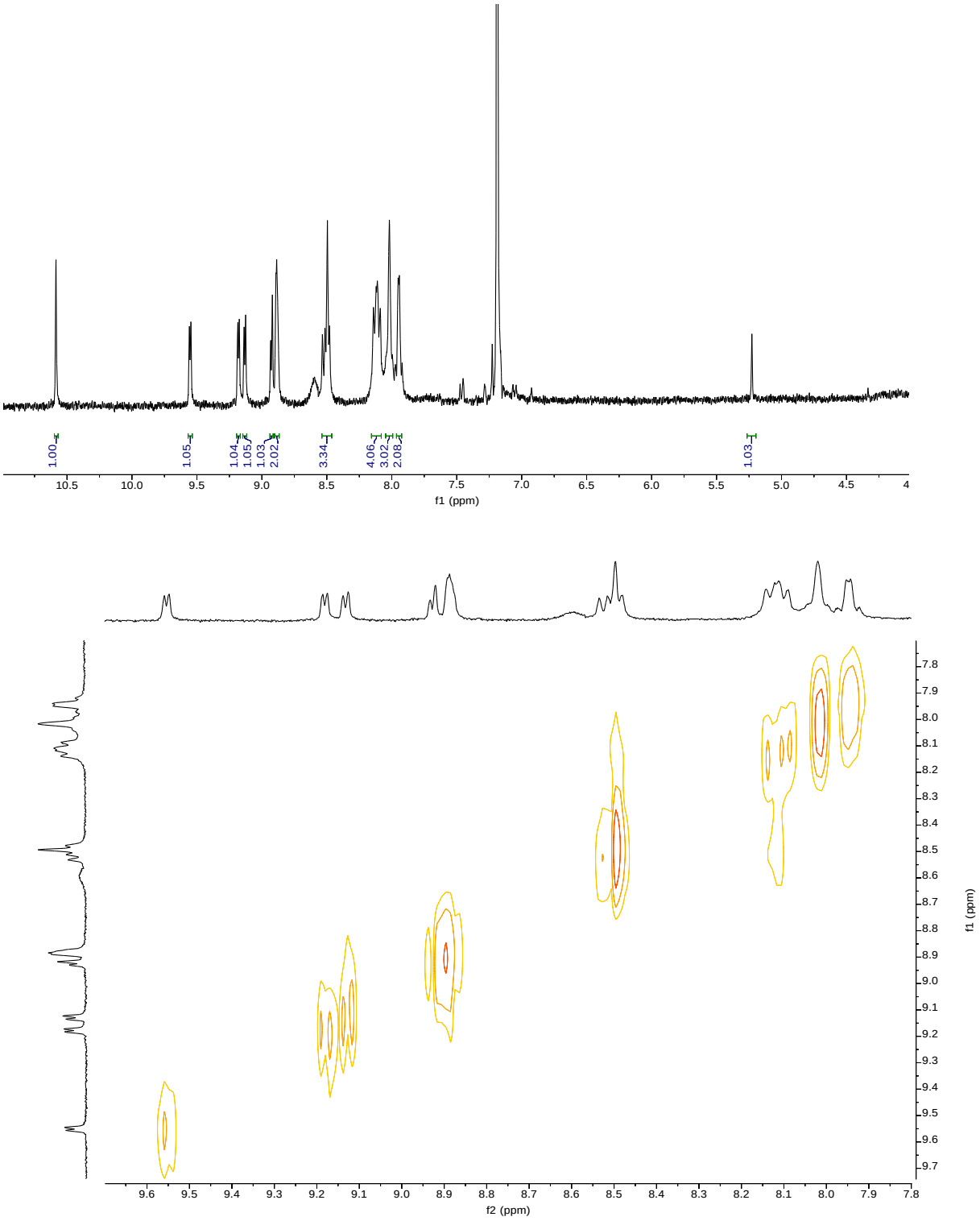

Figure S38. ^{1}H NMR and ^{1}H—^{1}H COSY spectra of Re[T*p*CF$_3$PC-3-(CN)COOH](O) in $CDCl_3$ at 20°C.

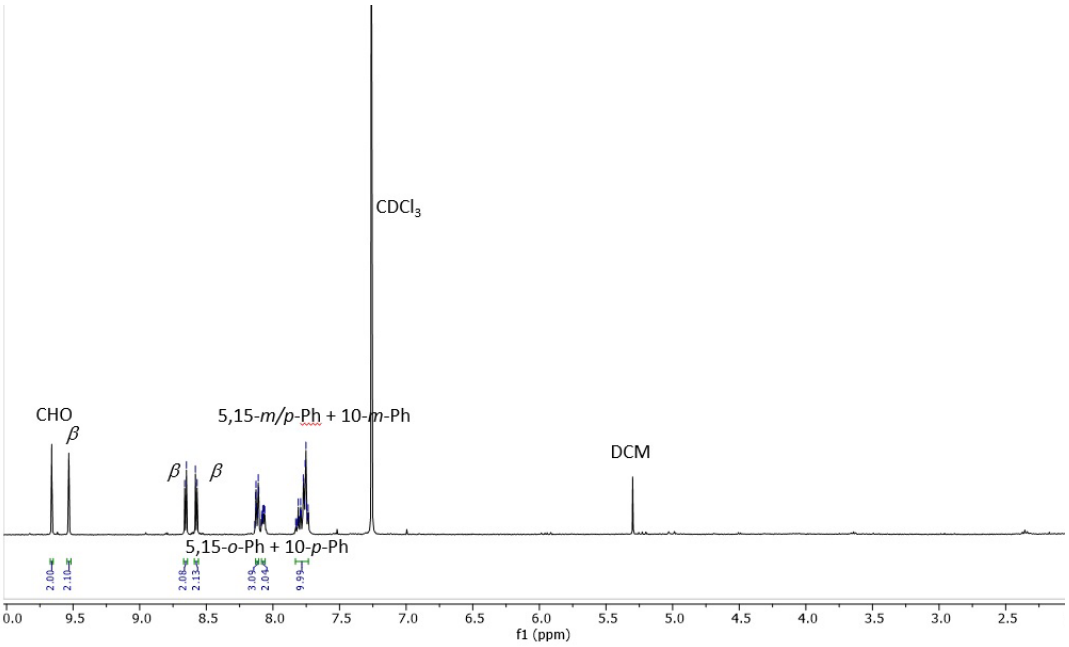

Figure S39. ^{1}H NMR spectrum of Au[TPC-3,17-(CHO)$_2$] in $CDCl_3$ at -20°C.

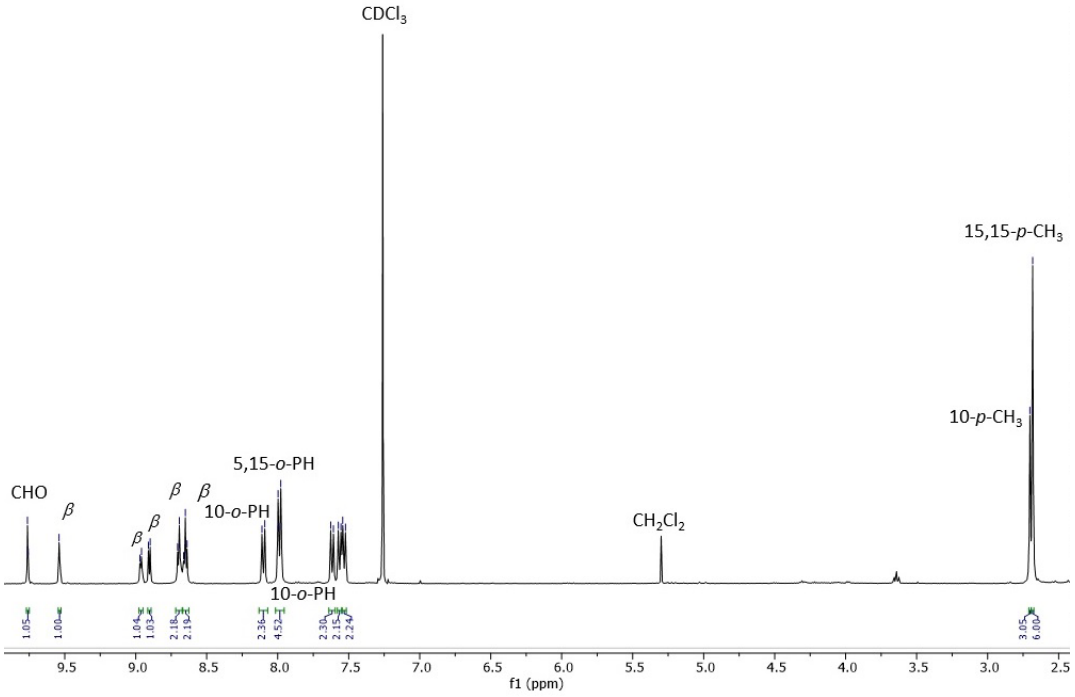

Figure S40. ^{1}H NMR spectrum of Au[T*p*CH$_3$PC-3-CHO] in $CDCl_3$ at -20°C.

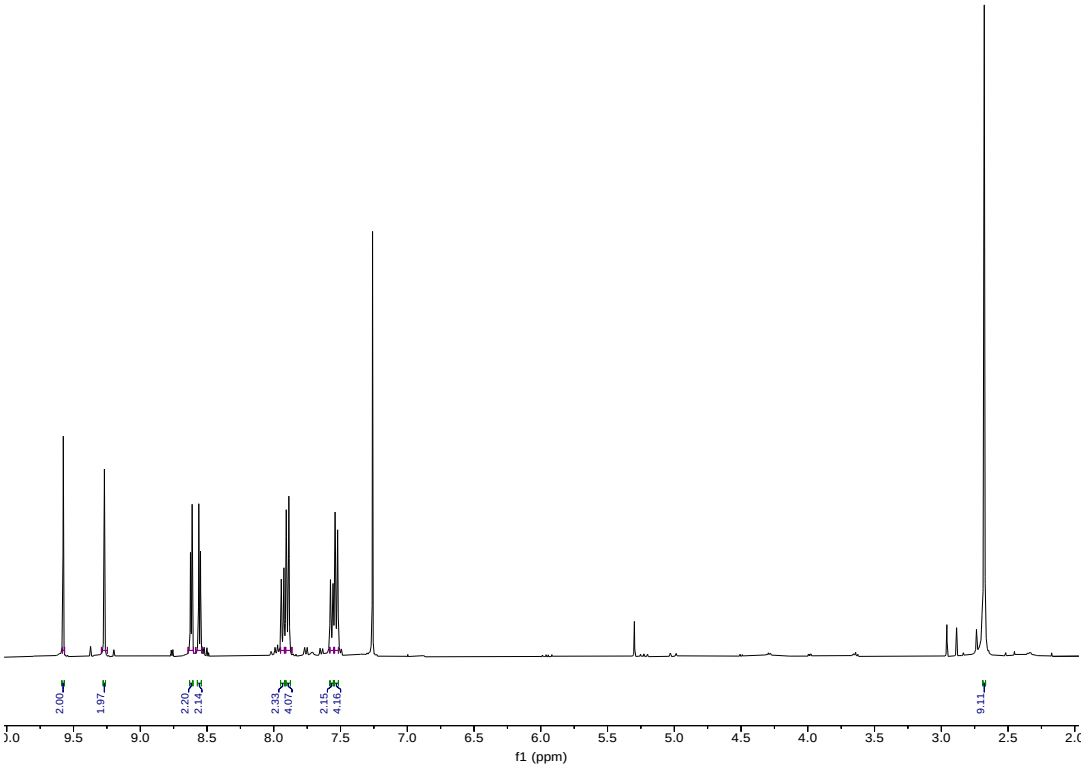

Figure S41. ^{1}H NMR spectrum of Au[T*p*CH_3PC-3,17-$(CHO)_2$] in $CDCl_3$ at -20°C.

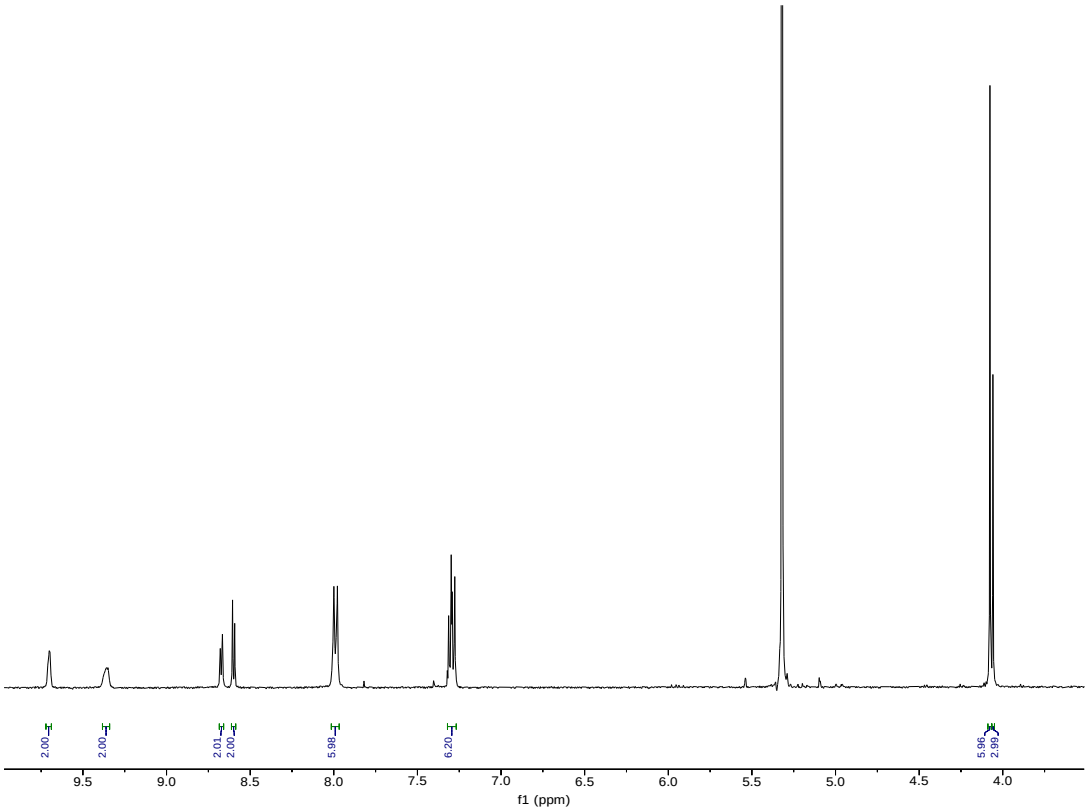

Figure S42. ^{1}H NMR spectrum of Au[T*p*OCH_3PC-3,17-$(CHO)_2$] in $CDCl_3$ at -20°C.

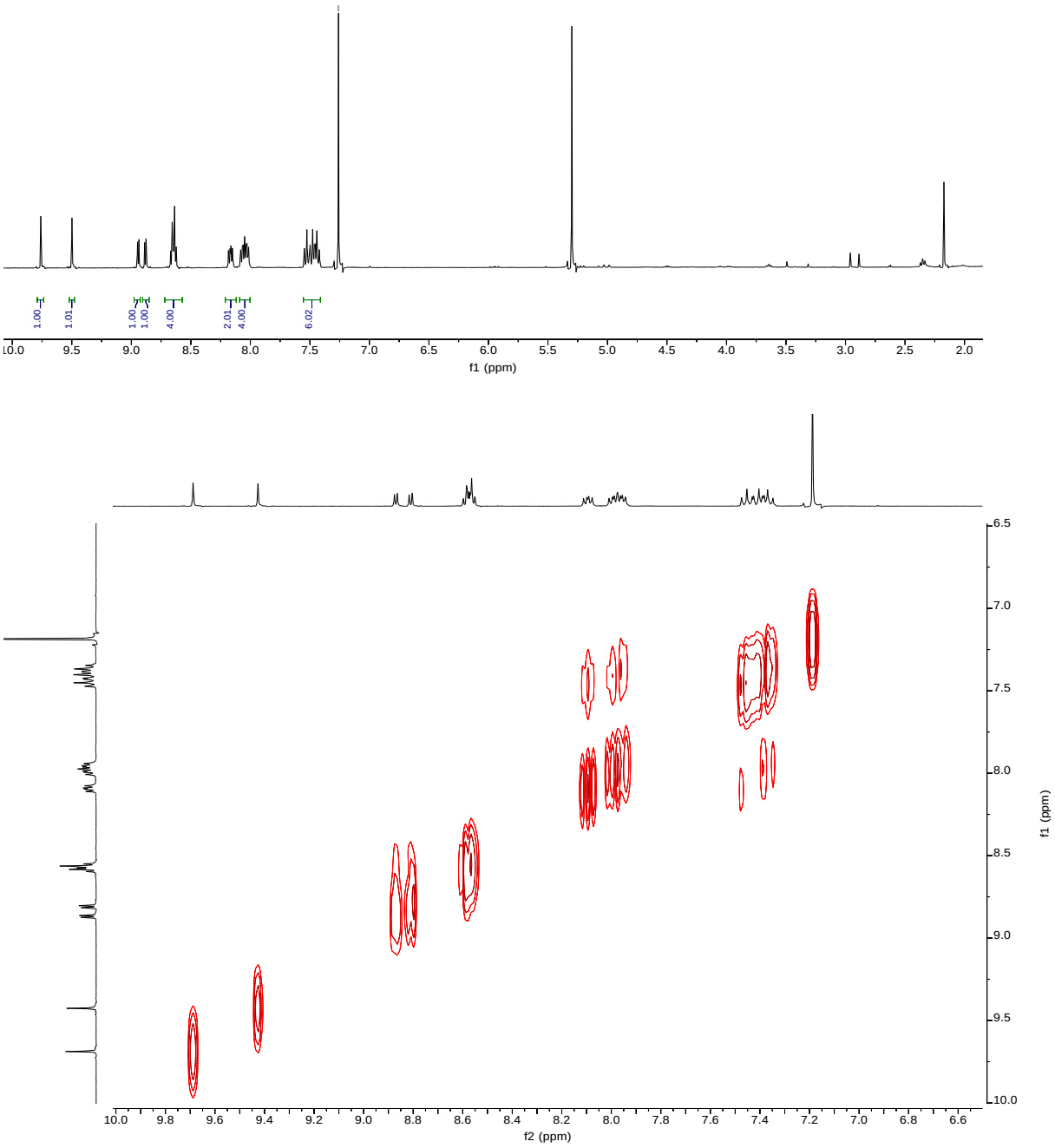

Figure S193. ^{1}H NMR and ^{1}H—^{1}H COSY spectra of Au[T*p*FPC-3-CHO] in $CDCl_3$ at 20°C.

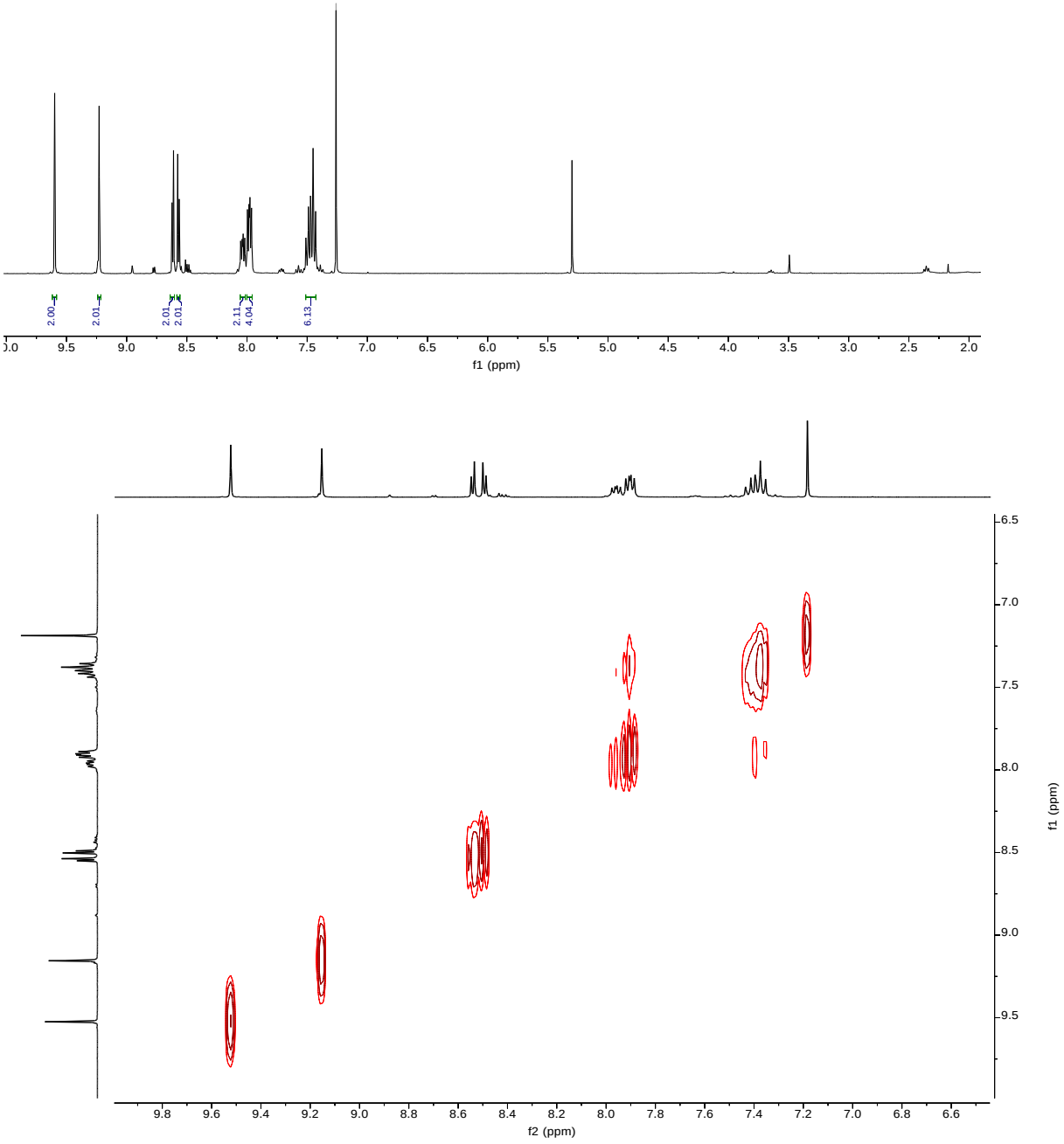

Figure S44. ^{1}H NMR and ^{1}H—^{1}H COSY spectra of Au[T*p*FPC-3,17-$(CHO)_2$] in $CDCl_3$ at 20°C.

D. Partial characterization of minor products

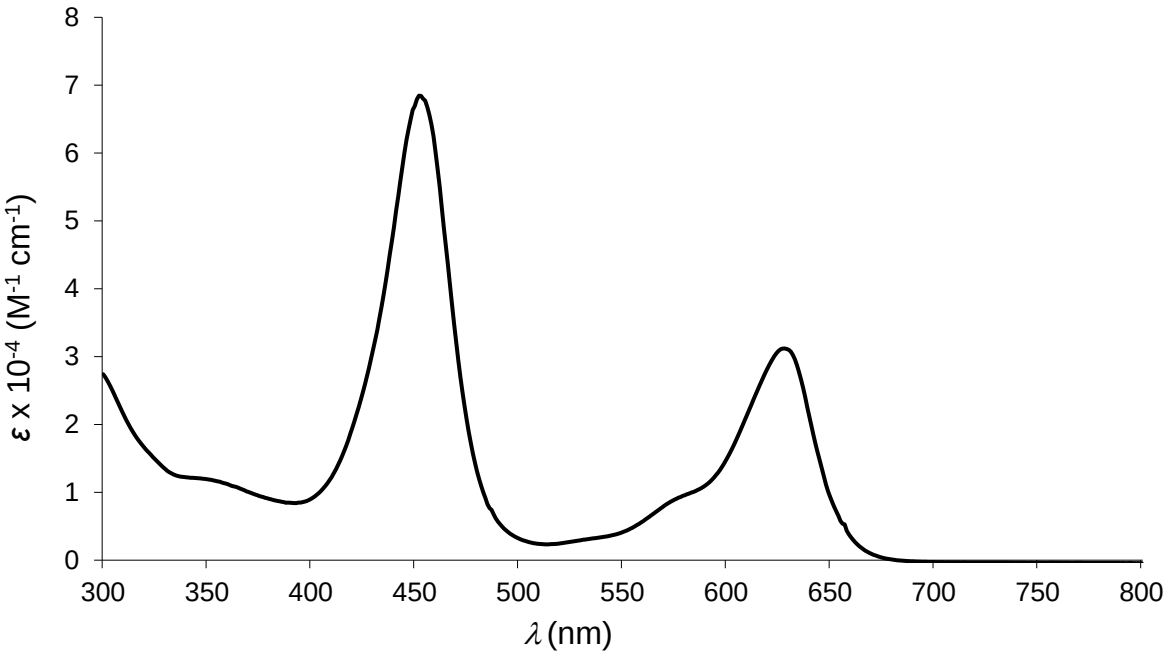

Figure S45. UV-vis spectrum of Re[T*p*CH_3PC-3,17-$(CHO)_2$] in dichloromethane.

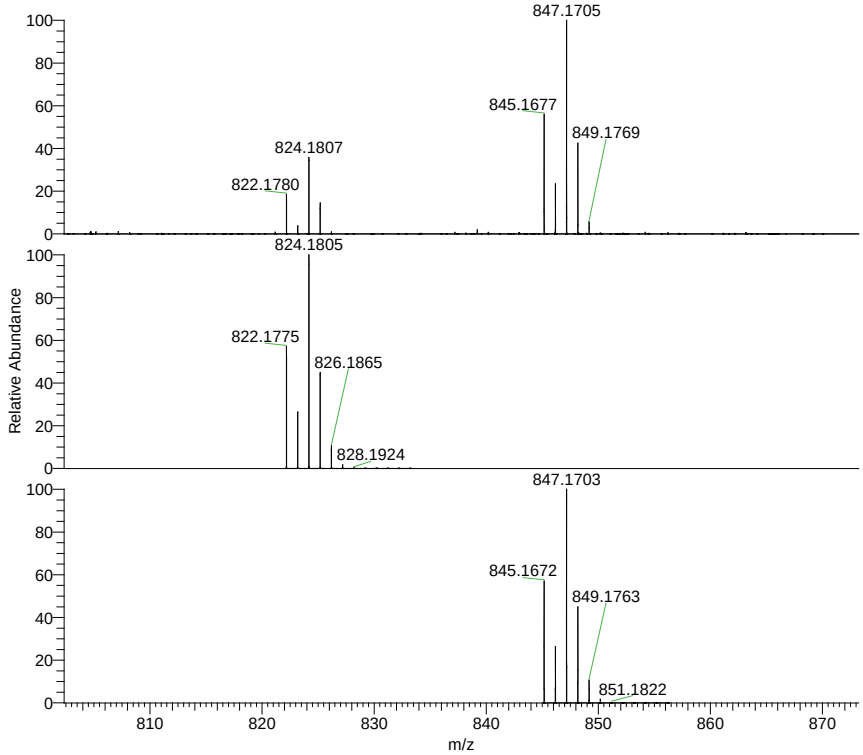

Figure S46. ESI mass spectrum of Re[T*p*CH_3PC-3,17-$(CHO)_2$](O).

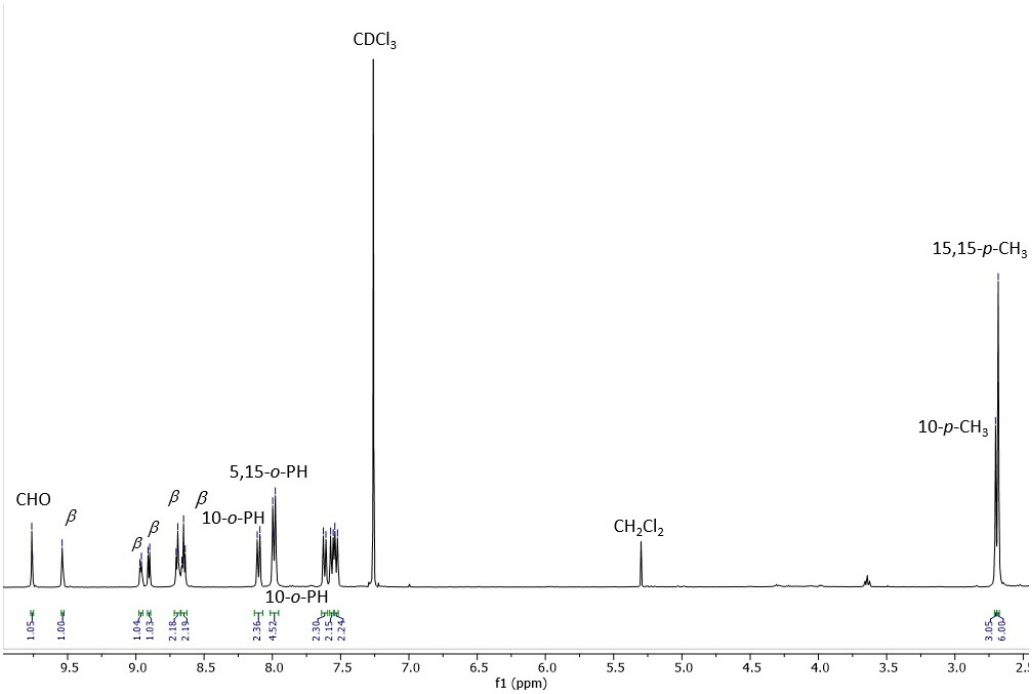

Figure S47. ^{1}H NMR spectrum of Au[T*p*CH$_3$PC-3-CHO] in CDCl$_3$ at -20°C.

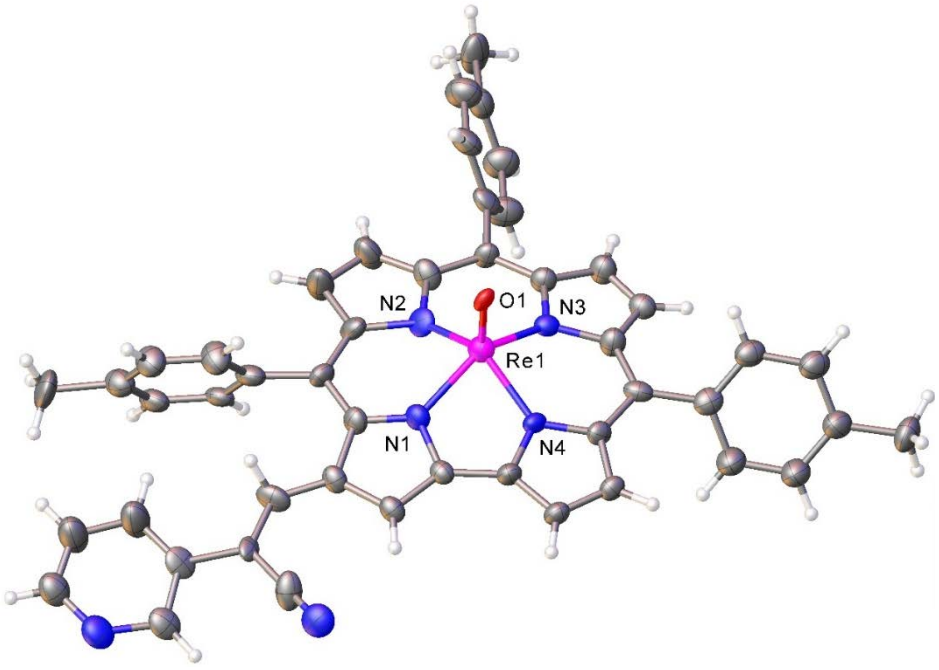

Figure S48. Thermal ellipsoid plot for the Knoevenagel condensate of Re[T*p*CH$_3$PC-3-CHO] with pyridin-3-ylacetonitrile. Selected distances (Å): Re1-N1 2.003(18), Re1-N2 1.87(2), Re1-N3 1.973(18), Re1-N4 1.956(16). Re(1)-N(3) 1.973(18) Re(1)-N(4) 1.956(16). The relatively poor quality of the structure implies that it should be only as proof of connectivity.